J|A|C|S
ARTICLES
Published on Web 05/01/2004

Subphthalocyanines: Tuneable Molecular Scaffolds for Intramolecular Electron and Energy Transfer Processes

David González-Rodríguez,[†] Tomás Torres,*[,†] Dirk M. Guldi,*[,‡] José Rivera,[§,||] Maria Ángeles Herranz,[§] and Luis Echegoyen*[,§]

Contribution from the Departamento de Química Orgánica, Facultad de Ciencias, Universidad Autónoma de Madrid, E-28049 Madrid, Spain; the Radiation Laboratory, University of Notre Dame, Indiana 46556; and the Department of Chemistry, Clemson University, South Carolina 29634

Received December 1, 2003; E-mail: tomas.torres@uam.es; guldi.1@nd.edu; luis@clemson.edu

Abstract: A series of four subphthalocyanine−C_{60} fullerene dyads have been prepared through axial functionalization of the macrocycle with *m*-hydroxybenzaldehyde and a subsequent dipolar cycloaddition reaction. The subphthalocyanine moiety has been peripherally functionalized with substituents of different electronic character, namely fluorine or iodine atoms and ether or amino groups, thus reaching a control over its electron-donating properties. This is evidenced in cyclic voltammetry experiments by a progressive shift to lower potentials, by ca. 200 mV, of the first oxidation event of the SubPc unit in the dyads. As a consequence, the energy level of the SubPc$^{\bullet+}$−$C_{60}^{\bullet-}$ charge-transfer state may be tuned so as to compete with energy transfer deactivation pathways upon selective excitation of the SubPc component. For instance, excitation of those systems where the level of the radical pair lies high in energy triggers a sequence of exergonic photophysical events that comprise (i) nearly quantitative singlet−singlet energy transfer to the C_{60} moiety, (ii) fullerene intersystem crossing, and (iii) triplet−triplet energy transfer back to the SubPc. On the contrary, the stabilization of the SubPc$^{\bullet+}$−$C_{60}^{\bullet-}$ radical pair state by increasing the polarity of the medium or by lowering the donor−acceptor redox gap causes charge transfer to dominate. In the case of **1c** in benzonitrile, the thus formed radical pair has a lifetime of 0.65 ns and decays via the energetically lower lying triplet excited state. Further stabilization is achieved for dyad **1d**, whose charge-transfer state would lie now below both triplets. The radical pair lifetime consequently increases in more than 2 orders of magnitude with respect to **1c** and presents a significant stabilization in less polar solvents, revealing a low reorganization energy for this kind of SubPc−C_{60} systems.

Introduction

Conversion of solar energy into profitable chemical energy in natural photoactive centers involves three primary sequential photochemical events: light absorption, excitation energy transduction, and photoinduced electron transfer.[1] The optimization of each of these key processes, as well as the comprehension of their mutual interplay, is of paramount importance for the development of efficient nature-mimicking photosynthetic systems,[2] the ultimate goal being the processing of light into other energy sources, chemical[3] or electrical equivalents,[4] or into information bits.[5]

In such synthetic systems, C_{60} fullerenes have been widely employed as the electron-acceptor unit, due to their unique redox[6] and structural[7] properties. On the other hand, the prominent ground-state absorption in the visible region of the spectrum of π-conjugated macrocycles, such as porphyrins and phthalocya-

[†] Universidad Autónoma de Madrid.
[‡] University of Notre Dame.
[§] Clemson University.
[||] Current address: Department of Chemistry, Pontificial Catholic University, Ponce, Puerto Rico 00731. E-mail: jorivera@pucpr.edu

(1) (a) Feher, G.; Allen, J. P.; Okamura, M. Y.; Rees, D. C. *Nature* **1989**, *339*, 111−116. (b) Deisenhofer, J.; Michel, H. *Angew. Chem., Int. Ed. Engl.* **1989**, *28*, 872−892. (c) Huber, R. *Angew. Chem., Int. Ed. Engl.* **1989**, *28*, 849−871. (d) *The Photosynthetic Reaction Center*; Deisenhoifer, J.; Norris, J. R., Eds.; Academic Press: New York, 1993. (e) *Molecular Mechanisms of Photosynthesis*; Blankenship, R. E., Ed.; Blackwell Science, 2002.
(2) (a) Balzani, V.; Scandola, F. *Supramolecular Photochemistry*; Ellis Horwood: Chichester, U.K., 1991; pp 161−196, 355−394. (b) Turro, N. J. *Modern Molecular Photochemistry*; University Science Books: Mill Valley, CA, 1991; pp 321−361. (c) Speiser, S. *Chem. Rev.* **1996**, *96*, 1953−1976.
(3) (a) Gust, D.; Moore, T. A.; Moore, A. L.; Lee, S.-J.; Bittersmann, E.; Luttrull, D. K.; Rehms, A. A.; DeGraziano, J. M.; Ma, X. C.; Gao, F.; Belford, R. E.; Trier, T. T. *Science* **1990**, *248*, 199−201. (b) Gust, D.; Moore, T. A.; Moore, A. L.; Macpherson, A. N.; Lopez, A.; DeGraziano, J. M.; Gouni, I.; Bittersmann, E.; Seely, G. R.; Gao, F.; Nieman, R. A.; Ma, X. C.; Demanche, L. J.; Hung, S.-C.; Luttrull, D. K.; Lee, S.-J.; Kerrigan, P. K. *J. Am. Chem. Soc.* **1993**, *115*, 11141−11152. (c) Bennett, I. M.; Farfano, H. M. V.; Bogani, F.; Primak, A.; Liddell, P. A.; Otero, L.; Sereno, L.; Silber, J. J.; Moore, A. L.; Moore, T. A.; Gust, D. *Nature* **2002**, *420*, 398−401.
(4) (a) Yu, G.; Gao, J.; Hummelen, J. C.; Wudl, F.; Heeger, A. J. *Science*, **1995**, *270*, 1789−1791. (b) Granström, M.; Petritsch, K.; Arias, A. C.; Lux, A.; Andersson, M. R.; Friend, R. H. *Nature*, **1998**, *395*, 257−260. (c) Brabec, C.; Sariciftci, N. S.; Hummelen, J. C. *Adv. Funct. Mater.* **2001**, *11*, 15−26.
(5) (a) Balzani, V.; Credi, A.; Raymo, F. M.; Stoddart, J. F. *Angew. Chem., Int. Ed.* **2000**, *39*, 3348−3391. (b) Balzani, V.; Credi, A.; Venturi, M. in *Stimulating Concepts in Chemistry;* Vögtle, F.; Stoddart, J. F.; Shibasaki, M., Eds.; Wiley-VCH: Weinheim, 2000.
(6) Echegoyen, L.; Echegoyen, L. E. *Acc. Chem. Res.* **1998**, *31*, 593−601.
(7) (a) *The Chemistry of the Fullerenes*; Hirsch, A., Ed.; Georg Thieme Verlag: Stuttgart, 1994. (b) *Science of Fullerenes and Carbon Nanotubes*; Dresselhaus, M. S.; Dresselhaus, G.; Eklund, P. C. Academic Press: San Diego, 1996. (c) *Fullerenes: from Synthesis to Optoelectronic Properties*; Guldi, D. M.; Martín, N., Eds.; Kluwer Academic Publishers: Dodrech, 2002.

nines,[8] together with their rich redox chemistry, provides both excellent light-harvesting and electron-donor performances. In addition, porphyrin−[9] or phthalocyanine−C_{60}[10] arrays commonly retain the characteristic low reorganization energies of fullerenes and are therefore ideally suited for the high-yield generation of long-lived charge-separated radical ion pairs.

Though these planar aromatic molecules have been the subject of extensive research in this field, the potential of subphthalocyanines (SubPcs),[11] the singular lower analogues of phthalocyanines, as active components in chemically/electronically coupled systems is yet to be determined. Despite their early discovery in 1972,[12] the interest of the scientific community in SubPcs actually arose in the 1990s, originally as synthetic precursors of unsymmetrically substituted phthalocyanines,[13] as first described by Kobayashi and co-workers, and then in view of their remarkable structural[14,15] and physical properties.[16−19] SubPcs are 14 π-electron aromatic macrocycles that comprise three *N*-fused diiminoisoindole units and an axial ligand around a tetracoordinated boron atom. Accordingly, these molecules render a C_3-symmetrical cone-shaped structure[14] that may give rise to chirality when appropriately substituted.[15]

Within the context of solar energy conversion, the strong fluorophore features that SubPcs display in the visible are promising means for efficient light harvesting. In particular, intense *Q*-band transitions, in the 550−650 nm region, whose extinction coefficients are on the order of ∼50.000 M^{-1} cm^{-1} clearly outscore those of porphyrins and metalloporhyrins. Their high electronic excitation energy, exceeding 2.0 eV, is conceived to power a strongly exergonic electron transfer, which subsequently intercedes the conversion between light and chemical/electrical energy. Moreover, the rigid nonplanar SubPc core affords small Stokes shifts and very low reorganizational energies,[19a] which are both fundamental requisites for efficient intramolecular electron/energy transfer reactions. In conclusion, these characteristics render SubPcs a potential light-harvesting synthon for the integration into novel donor−acceptor arrays.

Because of the versatile chemistry of SubPcs,[11] their assembly into multicomponent photo- and electroactive systems may be performed via different routes involving peripheral[20] or axial functionalization.[14c−e,21] The axial approach bears the two-fold advantage that the macrocycle preserves its electronic characteristics, since the substitution pattern on the benzene rings remains unaltered, and that the preparation of unsymmetrically substituted SubPcs, which would lead to specific dyads, is not required. From our own experience, the exchange of the original halogen atom with oxygen nucleophiles, particularly phenols, is a very convenient method for increasing the solubility and stability of these molecules and, at the same time, for introducing diverse functional groups in the axial position of the ring.[21b]

We recently communicated the synthesis of SubPc−C_{60} dyads in which the two components were linked through isomeric *ortho*-, *meta*-, or *para*-substituted phenoxy spacers.[22] In these

(8) *The Porphyrin Handbook*; Kadish, K. M.; Smith, K. M.; Guillard, R., Eds.; Academic Press: San Diego, 2003.

(9) (a) Imahori, H.; Sakata, Y. *Adv. Mater.* **1997**, *9*, 537−546. (b) Prato, M. *J. Mater. Chem.* **1997**, *7*, 1097−1109. (c) Martín, N.; Sánchez, L.; Illescas, B.; Pérez, I. *Chem. Rev.* **1998**, *98*, 2527−2547. (d) Diederich, F.; Gómez-López, M. *Chem. Soc. Rev.* **1999**, *28*, 263−277. (e) Imahori, H.; Sakata, Y. *Eur. J. Org. Chem.* **1999**, 2445−2457. (f) Guldi, D. M. *Chem. Commun.* **2000**, 321−327. (g) Guldi, D. M.; Prato, M. *Acc. Chem. Res.* **2000**, *33*, 695−703. (h) Reed, C. A.; Bolskar, R. D. *Chem. Rev.* **2000**, *100*, 1075−1120. (i) Gust, D.; Moore, T. A.; Moore, A. L. *J. Photochem. Photobiol. B.* **2000**, *58*, 63−71. (j) Gust, D.; Moore, T. A.; Moore, A. L. *Acc. Chem. Res.* **2001**, *34*, 40−48. (k) Guldi, D. M. *Chem. Soc. Rev.* **2002**, *31*, 22−36. (l) Guldi, D. M.; Martín, N. *J. Mater. Chem.* **2002**, *12*, 1978−1992. (m) Meijer, M. D.; van Klink, G. P. M.; van Koten, G. *Coord. Chem. Rev.* **2002**, *230*, 141−163. (n) Guldi, D. M. *Pure Appl. Chem.* **2003**, *75*, 1069−1075. (o) Imahori, H.; Mori, Y.; Matano, Y. J. *Photochem. Photobiol. C* **2003**, *4*, 51−83.

(10) (a) Linssen, T. G.; Durr, K.; Hanack, M.; Hirsch, A. *J. Chem. Soc. Chem. Commun.* **1995**, 103−104. (b) Durr, K.; Fiedler, S.; Linssen, T.; Hirsch, A.; Hanack, M. *Chem. Ber.* **1997**, *130*, 1375−1378. (c) Sastre, A.; Gouloumis, A.; Vázquez, P.; Torres, T.; Doan, V.; Schwartz, B. J.; Wudl, F.; Echegoyen, L.; Rivera, J. *Org. Lett.* **1999**, *1*, 1807−1810. (d) Gouloumis, A.; Liu, S.-G.; Sastre, A.; Vázquez, P.; Echegoyen, L.; Torres, T. *Chem. Eur. J.* **2000**, *6*, 3600−3607. (e) Guldi, D. M.; Gouloumis, A.; Vázquez, P.; Torres, T. *Chem. Commun.* **2002**, 2056−2057. (f) Martínez-Díaz, M. V.; Fender, N. S.; Rodríguez-Morgade, M. S.; Gómez-López, M.; Diederich, F.; Echegoyen, L.; Stoddart, J. F.; Torres, T. *J. Mater. Chem.* **2002**, *12*, 2095−2099. (g) Guldi, D. M.; Ramey, J.; Martínez-Díaz, M. V.; de la Escosura, A.; Torres, T.; Da Ros, T.; Prato, M. *Chem. Commun.* **2002**, 2774−2775. (h) González-Rodríguez, D.; Torres T. in *The Exciting World of Nanocages and Nanotubes*; Kamat, P.; Guldi, D. M.; Kadish, K., Eds.; Proc. Electrochem. Soc., Fullerenes Vol. 12, pp 195−210, ECS: Pennington NJ, 2002.

(11) Claessens, C. G.; González-Rodríguez, D.; Torres, T. *Chem. Rev.* **2002**, *102*, 835−853.

(12) Meller, A.; Ossko, A. *Monatsh. Chem.* **1972**, *103*, 150−155.

(13) (a) Kobayashi, N.; Kondo, R.; Nakajima, S.-I.; Osa, T. *J. Am. Chem. Soc.* **1990**, *112*, 9640−9641. (b) Kasuga, K.; Idehara, T.; Handa, M. *Inorg. Chim. Acta* **1992**, *196*, 127−128. (c) Musluoglu, E.; Gürek, A.; Ahsen, V.; Gül, A.; Bekaroglu, Ö. *Chem. Ber.* **1992**, *125*, 2337−2339. (d) Dabak, S.; Gül, A.; Bekaroglu, Ö. *Chem. Ber.* **1994**, *127*, 2009−2012. (e) Weitemeyer, A.; Kliesch, H.; Wöhrle, D. *J. Org. Chem.* **1995**, *60*, 4900−4904. (f) Sastre, A.; Torres, T.; Hanack, M. *Tetrahedron Lett.* **1995**, *36*, 8501−8504. (g) Kudrevich, S. V.; Gilbert, S.; van Lier, J. E. *J. Org. Chem.* **1996**, *61*, 5706−5707. (h) Sastre, A.; del Rey, B.; Torres. T. *J. Org. Chem.* **1996**, *61*, 8591−8597. (i) Kobayashi, N.; Ishizaki, T.; Ishii, K.; Konami, H. *J. Am. Chem. Soc.* **1999**, *121*, 9096−9110.

(14) (a) Kietaibl, H. *Monatsh. Chem.* **1974**, *105*, 405−418. (b) Rauschnabel, J.; Hanack, M. *Tetrahedron Lett.* **1995**, *36*, 1629−1632. (c) Kasuga, K.; Idehara, T.; Handa, M.; Ueda, Y.; Fujiwara, T.; Isa, K. *Bull. Chem. Soc. Jpn.* **1996**, *69*, 2559−2563. (d) Engel, M. K.; Yao, J.; Maki, H.; Takeuchi, H.; Yonehara, H.; Pac, C. *Report Kawamura Inst. Chem. Res.* **1998**, *9* (*Vol. Date 1997*), 53−65. (e) Potz, R.; Göldner, M.; Hückstädt, H.; Cornelissen, U.; Tutaβ, A.; Homborg, H. *Z. Anorg. Allg. Chem.* **2000**, *626*, 588−596. (f) Claessens, C. G.; Torres, T. *Angew. Chem., Int. Ed.* **2002**, *41*, 2561−2564. (g) Fukuda, T.; Stork, J. R.; Potucek, R. J.; Olmstead, M. M.; Noll, B. C.; Kobayashi, N.; Durfee, W. S. *Angew. Chem., Int. Ed.* **2002**, *41*, 2565−2568.

(15) The two SubPc enantiomers, described by means of the helical descriptors M and P, have been separated by chiral HPLC. (a) Claessens, C. G.; Torres, T. *Tetrahedron Lett.* **2000**, *41*, 6361−6365. (b) Kobayashi, N.; Nonomura, T. *Tetrahedron Lett.* **2002**, *43*, 4253−4255.

(16) SubPcs have been considered as potential candidates in electrolithography or printing technologies. (a) Reynolds, S. J.; Gairns, R. S.; Simpson, P. A. (Zeneca Ltd.) PCT Int. Appl. WO 94,24,612, 1994 [*Chem. Abstr.* **1995**, *122*, 326420e]. (b) Enokida, T.; Suda, Y. (Toyo Ink Mfg Co, Japan) Japan Kokai Tokkyo Koho JP 07,102,251, 1995 [*Chem. Abstr.* **1995**, *123*, 69933g]. (c) Nohr, R. S.; MacDonald, J. G. (Kimberly-Clark Worldwide, Inc., USA) PCT Int. Appl. WO 0,071,621, 2000 [*Chem. Abstr.* **2001**, *134*, 18557].

(17) For high-density optical recording applications of SubPcs, see: (a) Wang, Y.; Gu, D.; Gan, F. *Opt. Commun.* **2000**, *183*, 445−450. (b) Wang, Y.; Gu, D.; Gan, F. *Phys. Status Solidi A* **2001**, *186*, 71−77. (c) See also the patents cited in ref 11.

(18) Nonlinear optical properties of SubPcs: (a) Díaz-García, M. A.; Agulló-López, F.; Sastre, A.; Torres, T.; Torruellas, W. E.; Stegeman, G. I. *J. Phys. Chem.* **1995**, *99*, 14988−14991. (b) Sastre, A.; Torres, T.; Díaz-García, M. A.; Agulló-López, F.; Dhenaut, C.; Brasselet, S.; Ledoux, I.; Zyss, J. *J. Am. Chem. Soc.* **1996**, *118*, 2746−2747. (c) Rojo, G.; Hierro, A.; Díaz-García, M. A.; Agulló-López, F.; del Rey, B.; Sastre, A.; Torres, T. *Appl. Phys. Lett.* **1997**, *70*, 1802−1804. (d) Rojo, G.; Agulló-López, F.; del Rey, B.; Torres, T. *J. Appl. Phys.* **1998**, *84*, 6507−6512. (e) del Rey, B.; Keller, U.; Torres, T.; Rojo, G.; Agulló-López, F.; Nonell, S.; Marti, C.; Brasselet, S.; Ledoux, I.; Zyss, J. *J. Am. Chem. Soc.* **1998**, *120*, 12808−12817. (f) Olbrechts, G.; Wostyn, K.; Clays, K.; Persoons, A.; Ho Kang, S.; Kim, K. *Chem. Phys. Lett.* **1999**, *308*, 173−175. (g) Olbrechts, G.; Clays, K.; Wostyn, K.; Persoons, A. *Synth. Met.* **2000**, *115*, 207−211. (h) Liang, Z.; Gan, F.; Sun, Z.; Yang, X.; Ding, L.; Wang, Z. *Opt. Mater. (Amsterdam)* **2000**, *14*, 13−17.

(19) Photophysical properties of SubPcs and derivatives: (a) Kipp, R. A.; Simon, J. A.; Beggs, M.; Ensley, H. E.; Schmehl, R. H. *J. Phys. Chem. A* **1998**, *102*, 5659−5664. (b) Nonell, S.; Rubio, N.; del Rey, B.; Torres, T. *J. Chem. Soc., Perkin Trans. 2* **2000**, 1091−1094. (c) Wrobel, D.; Boguta, A.; Mazurkiewicz, P. *Spectrochim. Acta, Part A* **2003**, *12*, 2841−2854.

(20) (a) del Rey, B.; Torres, T. *Tetrahedron Lett.* **1997**, *38*, 5351−5354. (b) Claessens, C. G.; Torres, T. *J. Am. Chem. Soc.* **2002**, *124*, 14522−14523.

(21) (a) Geyer, M.; Plenzig, F.; Rauschnabel, J.; Hanack, M.; del Rey, B.; Sastre, A.; Torres, T. *Synthesis* **1996**, 1139−1151. (b) Claessens, C. G.; González-Rodríguez, D.; del Rey, B.; Torres, T.; Mark, G.; Schuchmann, H.-P.; von Sonntag, C.; MacDonald, J. G.; Nohr, R. S. *Eur. J. Org. Chem.* **2003**, 2547−2551.

(22) González-Rodríguez, D.; Torres, T.; Guldi, D. M.; Rivera, J.; Echegoyen, L. *Org. Lett.* **2002**, *4*, 335−338.

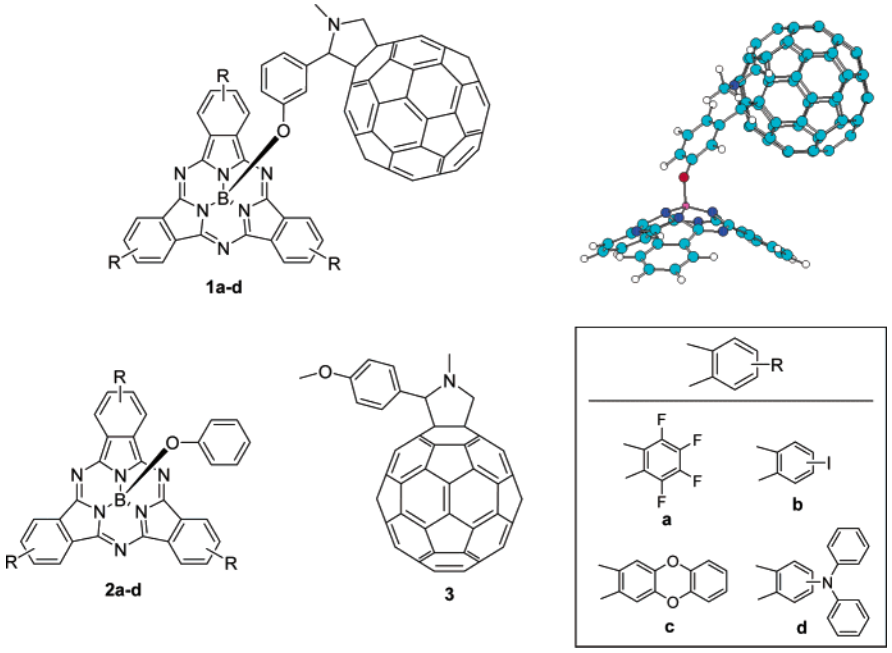

Figure 1. Structure and AM1-minimized model[24] of SubPc−C_{60} dyads **1a**−**d**, reference SubPcs **2a**−**d** and fulleropyrrolidine **3**.

Scheme 1. Synthesis of SubPc−C_{60} Dyads **1a**−**d**

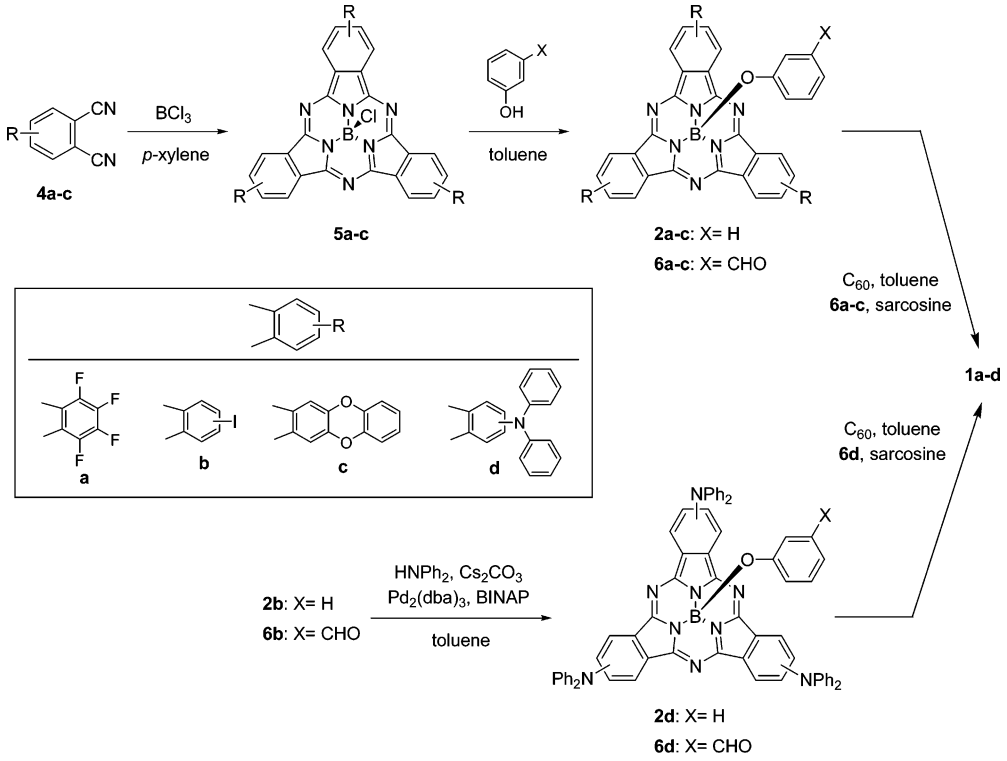

systems, we demonstrated a distance-dependent quenching of the SubPc fluorescence by singlet−singlet energy transfer to the fullerene unit. As one step further, we describe herein the effect of the modulation of the electronic properties of the macrocyclic moiety, while maintaining the same interchromophoric distance, on the electrochemical and photophysical properties of SubPc−C_{60} dyads (Figure 1). Thus, a *m*-disubstituted spacer was chosen as a compromise between the two other extreme *o*- and *p*-topologies,[22] and different peripheral groups (i.e., fluorine or iodine atoms and unprecedented ether or amino groups) were introduced in the SubPc core in order to control the competition between energy and electron-transfer phenomena to the fullerene.[23]

Results and Discussion

Synthesis. SubPcs **5a**−**c** (Scheme 1) were synthesized by condensation reaction of the corresponding phthalonitriles **4a**−**c** in the presence of boron trichloride, following a procedure

(23) (a) Guldi, D. M.; Luo, C.; Swartz, A.; Gómez, R.; Segura, J. L.; Martín, N.; Christoph, B.; Serdar, S. N. *J. Org. Chem.* **2002**, *67*, 1141−1152. (b) Guldi, D. M.; Swartz, A.; Luo, C.; Gómez, R.; Segura, J. L.; Martín, N. *J. Am. Chem. Soc.* **2002**, *124*, 10875−10886.

recently reported by us.[21b] So far, the high tendency of boron halides to cleave ether groups[25] precluded the synthesis of ether-substituted SubPcs from alkyloxyphthalonitriles.[26] We found, however, that the diphenyl ether moiety is stable enough to survive a BCl_3 cyclotrimerization and SubPc **5c** could be obtained in moderate yields (39%).

The axial chlorine atom in compounds **5a**−**c** was efficiently replaced with phenol derivatives heating a mixture of the corresponding SubPc and an excess of phenol (for **2a**−**c**) or 3-hydroxybenzaldehyde (for **6a**−**c**) in toluene. The reaction rate was found to be greatly dependent on the electronic nature of both the macrocycle and the phenol, decreasing for SubPcs bearing electron-withdrawing groups and for the formylphenol (see Experimental Section). So, in these conditions, the reaction between **5a** and 3-hydroxybenzaldehyde proceeded very slowly and the yield was improved using molten phenol as solvent.[21b]

With the aim of enhancing the donor ability of the macrocycle, the palladium-catalyzed cross-coupling methodology between amines and aryl halides, mainly developed in the groups of Buchwald and Hartwig,[27] was tested on triiodoSubPcs **2b** and **6b**. These reactions commonly employ a *tert*-butoxide base that, in our case, produced the rapid decomposition of the macrocycle. The substitution of this base by cesium carbonate,[27b,28] however, allowed for the first time the synthesis of amino-substituted SubPcs, which were obtained in excellent yields (87% (**2d**) and 82% (**6d**)) considering that three C−N bonds are being formed in one step. Despite this, any attempt to carry out this amination reaction directly on dyad **1b** was fruitless, in all cases recovering the starting material.[29]

SubPc−C_{60} dyads **1a**−**d** were prepared by a 1,3 dipolar cycloaddition reaction between formyl-substituted SubPcs **6a**−**d** and C_{60} in the conditions described by Prato.[30] Monoaddition products were isolated in moderate yields (∼45%), and in all cases, a small amount of bisadducts (∼8%) was also obtained. Fulleropyrrolidine **3** was synthesized from 4-methoxybenzaldehyde following a similar procedure.[31] In this instance, the formation of multiple-addition compounds was more significant, most probably due to the smaller steric effect of the aldehyde. Dyads **1a**−**d** are quite soluble in aromatic solvents (i.e., toluene, *o*-dichlorobenzene, benzonitrile) and carbon disulfide. In contrast to the starting SubPcs, they are sparingly soluble in other common organic solvents (i.e., acetone, CH_2Cl_2, $CHCl_3$). The presence of diphenylamino groups in the macrocyclic benzene rings increases notably the solubility of **1d** with respect to the other dyads.

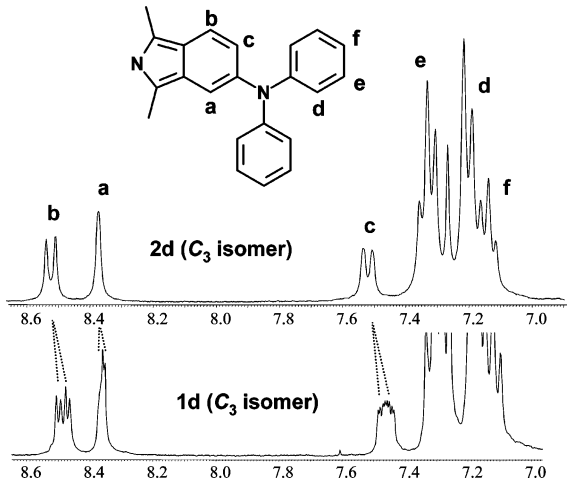

Figure 2. Aromatic portion of the ^1H NMR (300 MHz, $CDCl_3$) spectra of the C_3 regioisomers of **2d** and **1d**. The presence of a 1:1 mixture of diastereoisomers in **1d** is reflected in the splitting of some of the signals.

All the compounds were purified and characterized by ^1H NMR, ^{13}C NMR, UV−vis, FAB-MS or MALDI-TOF-MS, FT-IR, and elemental analysis. In the case of SubPcs **5b**, **2b** and **2d**, or dyads **1b** and **1d**, in which the macrocycle is trisubstituted, the corresponding C_3 and C_1 regioisomers could be separated by column chromatography and were individually characterized.[32] For the dyads, each of these isomers is constituted by a 1:1 mixture of diastereoisomers, since they possess two chiral elements: the subphthalocyanine itself[15] and the asymmetric carbon atom in the pyrrolidine ring. This is manifested by a clear splitting or broadening of some of the NMR proton signals, as illustrated in Figure 2 for the C_3 isomer of dyad **1d**. Unfortunately, we did not succeed in the chromatographic separation of these diastereoisomers. In ^1H NMR spectra (see Supporting Information), the effect of the aromatic macrocycle ring-current on the proton signals of the peripheral benzene rings, shifted downfield, and on those of the axial phenoxy spacer, that experience a significant shift to higher fields, should also be noted. In the latter case, the magnitude of the shift essentially depends on the distance of the protons to the core of the macrocycle and, to a lesser extent, on the electronic density of the π-system, being slightly more pronounced for the dodecafluoroSubPcs (series **a**).

Electrochemistry. The solution electrochemistry of SubPcs **2a**−**d** and SubPc-C_{60} dyads **1a**−**d** was investigated in THF under high vacuum conditions (see Experimental Section for details). The redox potentials obtained (vs ferrocene) are summarized in Table 1.

SubPcs **2a**−**d** exhibit several reduction peaks, with a reversible first reductive process that involves one electron (Figure 3). SubPcs **2a**, **c**, and **d** exhibit an additional reversible second reduction wave followed by an irreversible multiple-electron reduction wave (not shown for **2d**). This irreversibility seems to be due to chemical reactions following multiple-electron reductions.[22] An irreversible wave is generally observed between +372 and +1057 mV in the oxidative scan that seems to involve one electron. Additional waves are observed at +616 and +824 mV in the case of **2d**, the latter corresponding to a three-electron

(24) Structural modeling was performed using the Hyperchem 6.03 package (Hypercube, Inc.) for Windows.
(25) (a) Gerrard, W.; Lappert, M. F. *J. Chem. Soc.* **1952**, 1486−1490. (b) McOmie, J. F.; Watts, M. L.; West, D. E. *Tetrahedron*. **1968**, *24*, 2289−2292. (c) Bhatt, M. V.; Kulkarnyi, S. U. *Synthesis* **1983**, 249−282.
(26) The condensation of a crown-ether phthalonitrile in the presence of BPh_3 has been reported, but the macrocycle was isolated in a very low yield (<0.5%); see ref 13i.
(27) (a) Hartwig, J. F. *Angew. Chem., Int. Ed.* **1998**, *37*, 2046−2067. (b) Wolfe, J. P.; Wagaw, S.; Marcoux, J.-F.; Buchwald, S. L. *Acc. Chem. Res.* **1998**, *31*, 805−818. (c) Hartwig, J. F. *Acc. Chem. Res.* **1998**, *31*, 852−860. (d) Yang, B. H.; Buchwald, S. L. *J. Organomet. Chem.* **1999**, *576*, 125−146.
(28) Wolfe, J. P.; Buchwald, S. L. *Tetrahedron Lett.* **1997**, *38*, 6359−6362.
(29) This fact is not surprising, since fullerenes are known to efficiently coordinate Pd(0) species in a μ^2-fashion. For a general review, see: Balch, A. L.; Olmstead, M. M. *Chem. Rev.* **1998**, *98*, 2123−2165.
(30) (a) Maggini, M.; Scorrano, G.; Prato, M. *J. Am. Chem. Soc.* **1993**, *115*, 9798−9799. (b) Prato, M.; Maggini, M. *Acc. Chem. Res.* **1998**, *31*, 519−526. (c) Tagmatarchis, N.; Prato, M. *Synlett* **2003**, *6*, 768−779.
(31) (a) Zhou, D. J.; Gan, L. B.; Tan, H. S.; Luo, C. P.; Huang, C. H. *Chin. Chem. Lett.* **1995**, *6*, 1033−1036. (b) Jing, B.; Zhang, D.; Zhu, D. *Tetrahedron Lett.* **2000**, *41*, 8559−8563.
(32) The electrochemical and photophysical studies were performed, however, on a 1:3 mixture of C_3/C_1 regioisomers, due to their almost identical physical properties.

Table 1. Oxidation Peak Potentials and $E_{1/2}$ Data (THF, in mV vs Ferrocene) of SubPc−C_{60} Dyads **1a**−**d**, SubPcs **2a**−**d**, and Fulleropyrrolidine **3**

	$E^1_{pa,ox}$[a]	$E^2_{pa,ox}$[a]	$E^3_{pa,ox}$[a]	$E^1_{1/2,red}$[b]	$E^2_{1/2,red}$[b]	$E^3_{1/2,red}$[b]
2a	+1057			−1088	−1690	
2b	+821			−1323		
2c	+600			−1511	−2051	
2d[c]	+374	+616	+824 (3e)	−1579	−2079	
1a	+1047			−1053 (2e)	−1554	−1675
1b	+779	+998		−1004	−1347	−1511
1c	+645			−1032	−1528 (2e)	−2220
1d[c]	+372	+586	+840 (3e)	−1017	−1532 (2e)	−2162
3				−910	−1432	−2019

[a] Since these oxidative processes are irreversible, only anodic peak potentials are reported. [b] Reversible reduction processes. Standard electrode potentials are reported. [c] A gold electrode was used as the working electrode.

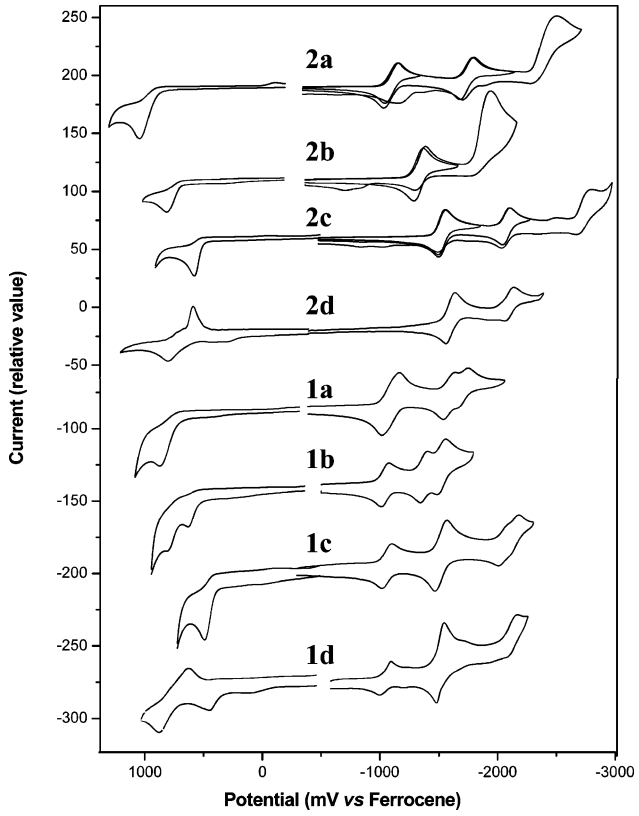

Figure 3. Cyclic voltammograms of SubPcs **2a**−**d** and dyads **1a**−**d** in THF and 0.1 M $TBAPF_6$ as supporting electrolyte.

process due to the oxidation of the diphenylamino groups in the SubPc.[33] After a full anodic scan, strong adsorption occurred in the working electrode, especially evident for amino-substituted compounds, which seems to be the cause of this irreversibility.

The nature of the peripheral substituents on the macrocycle modify strongly the reduction and oxidation potentials of the subphthalocyanines. The redox potentials follow the trend one would anticipate from the substitution pattern, the amino derivative **2d** being the easiest to oxidize ($E^1_{pa,ox} = +374$ mV), followed by the oxo derivative **2c** ($E^1_{pa,ox} = +600$ mV) and finally the SubPcs featuring iodo and fluoro substituents **2a** and **2b** ($E^1_{pa,ox} = +821$ and +1057 mV, respectively). The reduction potentials follow the same trend. Remarkably, **2d** is the most easily oxidized subphthalocyanine reported thus far.[11]

(33) Liu, S.-G.; Shu, L.; Rivera, J.; Liu, H.; Raimundo J.-M.; Roncali, J.; Gorgues, A.; Echegoyen, L. *J. Org. Chem.* **1999**, *64*, 4884−4886.

Table 2. Kinetic and Spectroscopic Features of Photoexcited and One-Electron Oxidized SubPc References **2a**−**d** in Toluene

feature	2a	2b	2c	2d
absorption maximum, nm	573	571	570	618
fluorescence maximum, nm	585	585	585	650
fluorescence quantum yield	0.4	0.08	0.49	0.15
fluorescence lifetime, ns	1.66	0.51	1.76	1.5
phosphorescence maximum[a], nm	835	835	844	>850
singlet excited-state maximum, nm	660	650	675	730
singlet excited-state lifetime, ns	1.73	0.59	1.81	1.26
s^{-1}	5.8×10^8	1.7×10^9	5.5×10^8	7.9×10^8
triplet excited-state maximum, nm	460	460	480	550
triplet excited-state lifetime, μs	28	32	36	40
radical cation maximum[b], nm	620	620	620	685

[a] In methylcyclohexane, 2-methyltetrahydrofuran, ethyliodide (2:1:1 v/v). [b] In dichloromethane.

Dyads **1a**−**d** essentially retain the anodic electrochemical pattern of both the parent [60]fullerene and SubPcs **2a**−**d** (Figure 3). However, the irreversible oxidation potentials are, in general, shifted to less positive values when compared to those of SubPcs **2a**−**d** (Table 1).

On the reduction scan, the waves can be assigned to the C_{60} or to the subphthalocyanine core. The first reversible reduction waves are assigned in all the cases to the C_{60} core. For **1a** ($E^1_{1/2,red} = -1053$ mV), this wave corresponds to a two-electron process, since it overlays with the first reduction of the subphthalocyanine moiety. In **1b**, the reduction of both fragments is clearly distinguished, but this is not the case for dyads **1c** and **1d**, where again, the second reduction wave is a two-electron process, which involves the second reduction of the C_{60} core and the first reduction of the oxo- or amino-SubPcs ($E^1_{1/2,red} = -1528$ and −1532 mV, respectively). Dyad **1b** seems to be the easiest to reduce in the series (by ca. 15 mV), but electrochemically, no ground-state interactions between both electroactive units are observed in these dyads.

Photophysics. Because of the diverse oxidation potentials that the newly synthesized SubPc moieties exhibit (vide supra), we tested donor−acceptor dyads **1a**−**d** by means of various photolytic techniques (i.e., steady-state and time-resolved) and compared their transient behavior with the excited-state properties featured by the adequate references, that is, SubPcs **2a**−**d**, which are summarized in Table 2, and fullerene **3**.

SubPc References 2a−d. Despite the different substituents, placed on the periphery of the SubPc core, **2a**−**c** reveal nearly superimposable singlet ground-state transitions. Soret-band like absorptions are typically seen at 330 nm, while the energetically lower lying *Q*-bands appear at 570 nm (Figure 4). This leads to the conclusion that the SubPc substituent has little impact on the $S_0 \rightarrow S_2$ and $S_0 \rightarrow S_1$ energy gaps. The only exception is **2d**, whose transitions are considerably red-shifted (i.e., *Q*-band maximum at 618 nm) bringing about marked changes in color from the typical intense magenta (**2a**−**b**) to green (**2d**). SubPcs **2c** and **2d** present an additional broad band around 450 nm, which is attributed to $n-\pi^*$ transitions.

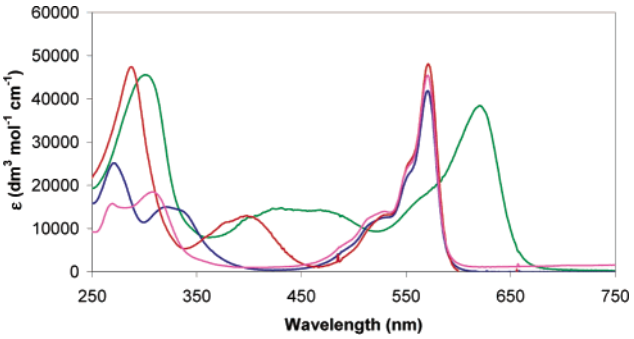

Figure 4. UV−vis spectra of SubPcs **2a** (pink), **2b** (blue), **2c** (red), and **2d** (green) in $CHCl_3$.

The substitution pattern that the reference SubPcs bear, including heavy atom providing iodine, on the other hand, exerts notable effects on the fluorescing features (i.e., $\lambda_{max} = 585$ nm). For example, diverse fluorescence quantum yields of the SubPc emission were detected in room-temperature experiments, which are as low as 0.08 (**2b**) but reach up to 0.49 (**2c**). From the 585 nm fluorescence maxima, we derive singlet excited state energies of 2.1 eV. It is important to note that these values are substantially and slightly higher than those seen for phthalocyanines (∼1.7 eV) and porphyrins (∼2.0 eV), respectively.[8] The fluorescence lifetimes, another radiative property, paralleled the aforementioned fluorescence quantum yields. Hereby a good correlation was established between these two radiative parameters; that is, higher quantum yields coincide always with longer lifetimes. Again **2d** is different, with a rather low singlet excited-state energy of 1.9 eV.

Since we are concerned with determining the excited-state energy levels of these novel chromophores, we complemented the emission assay with phosphorescence measurements in the reference SubPcs **2a**−**d**. These inherently weak features, with room-temperature quantum yields well below our $\sim 10^{-6}$ detection limit, necessitated working at low temperature (i.e., frozen glass matrix) and with the help of ethyliodide, a classical heavy atom provider. As a result, the fluorescent SubPc singlet excited state, emitting around 585 nm, was qualitatively abolished. Instead, a new emitting transition, located in the near-infrared region (i.e., 835 nm −**2b**), was registered. We ascribe the latter to the phosphorescent triplet state (see Figure S1 in Supporting Information). Based on these maxima, we derive triplet energies of 1.45 eV, in accordance with previous studies that set an upper limit for this energy level of 1.7 eV.[18e] Considering singlet−triplet energy gaps of ca. 0.65 eV in subphthalocyanines, we notice an evident trend towards larger gaps relative to phthalocyanines (0.2 eV) and porphyrins (0.5 eV). For **2d**, the phosphorescence lies outside of our detection limit, which shifts its triplet energy below 1.45 eV.

In terms of nonfluorescing singlet−singlet transitions, all the singlet excited states display, besides their strong bleaching in the Q-band region, characteristic features in the far visible. For example, following a 18 ps laser pulse, photoexcitation of **2a**−**d** led to the instantaneous formation of sharp maxima in the 620−750 nm region; see Figure 5a. Typically, these transients are short-lived with decay dynamics that obey to a monoexponential rate law, yielding rates on the order of 10^9 s^{-1}. While the absorption changes in the near-infrared are governed by the disappearance of the singlet−singlet absorption, simultaneous formation of new maxima, typically around 450 nm, were noted

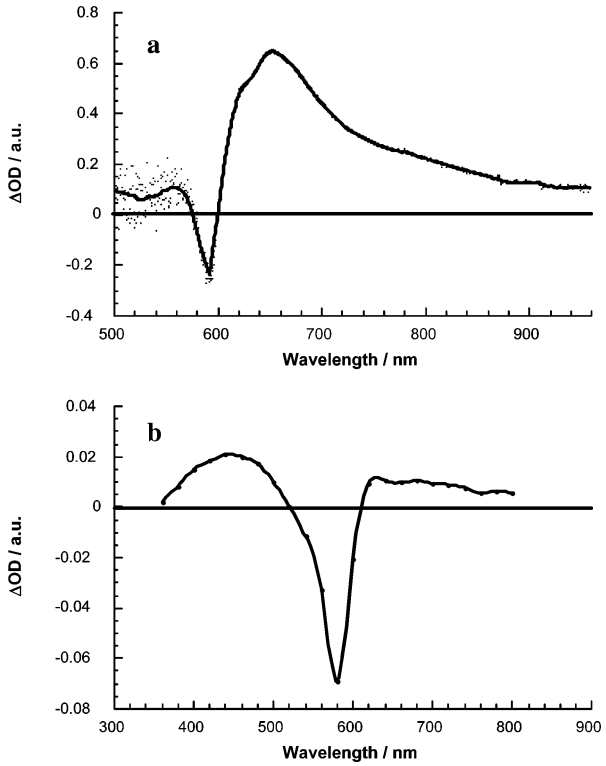

Figure 5. Differential absorption spectra obtained (a) upon picosecond flash photolysis (532 nm) and (b) upon nanosecond flash photolysis (532 nm) of ∼1.0×10^{-5} M solutions of SubPc **2b** in nitrogen saturated toluene with a time delay of 25 ps and 50 ns, respectively.

in the blue region, similar to the features shown in Figure 5b. Particularly important are the nearly identical time constants of the decay (**2a**: 5.8×10^8 s^{-1}) and growth (**2a**: 4.5×10^8 s^{-1}) processes, which leads consequently to the conclusion that a spin-forbidden intersystem crossing (ISC) to the energetically lower-lying triplet excited-state prevails. It is worthwhile to underline that the kinetics of ISC reveal a strong resemblance with the fluorescence dynamics.

An additional test in support of the ISC hypothesis required examining the triplet absorption characteristics in nanosecond experiments, for example, following 10 ns pulses at 532 nm. In this context, probing similar solutions in nanosecond experiments allowed the confirmation of the picosecond experiments. In fact, the triplet−triplet maxima were, as shown in Figure 5b, in perfect accord with the spectral features observed at the end of the picosecond time scale.

In addition to characterizing the ground and excited states of SubPcs **2a**−**d**, we examined the differential absorption changes of their oxidized states as well. More specifically, we subjected solutions of approximately 5.0×10^{-5} M of **2a**−**d** to pulse radiolytic oxidation in oxygenated dichloromethane. In short, these pulse radiolysis conditions lead to the instantaneous formation of the solvent radical cations (i.e., $[CH_2Cl_2]^{\bullet+}$) and the associated peroxyl radicals (i.e., $^{\bullet}OOCH_2Cl/^{\bullet}OOCHCl_2$).[34] Both are known to initiate the selective one-electron oxidation of macrocyclic systems, including porphyrins, phthalocyanines, and so forth. In this light, we ascribe the differential absorption changes to the one-electron oxidized π-radical cation (see Figure S2 in Supporting Information). Important attributes are, besides

(34) Shank, N. E.; Dorfman, L. M. *J. Chem. Phys.* **1970**, *52*, 4441−4447.

Table 3. Photophysical Parameters of SubPc−C_{60} Dyads **1a**−**d**

feature	solvent	1a	1b	1c	1d
fluorescence maximum, nm	toluene	588	592	588	655
fluorescence quantum yield (SubPc)	toluene	1.2×10^{-3}	9.6×10^{-4}	3.1×10^{-3}	1.1×10^{-3}
	ODCB	1.1×10^{-3}	1.0×10^{-3}	2.8×10^{-3}	7.8×10^{-4}
	bzcn	1.4×10^{-3}	9.6×10^{-4}	2.9×10^{-3}	5.1×10^{-4}
fluorescence quantum yield (C_{60})	toluene	5.0×10^{-4}	4.8×10^{-4}	4.9×10^{-4}	$<10^{-4}$
	ODCB	4.5×10^{-4}	4.7×10^{-4}	4.7×10^{-4}	
	bzcn	4.4×10^{-4}	3.9×10^{-4}	1.3×10^{-5}	
fluorescence lifetime (SubPc), ns	toluene	<0.1	<0.1	<0.1	0.25
	ODCB				0.22
	bzcn				0.2
fluorescence lifetime (C_{60}), ns	toluene	1.44	1.17	1.27	0.52
	ODCB	1.39	1.26	1.24	0.28
	bzcn	1.42	1.21	0.14	0.16
singlet excited-state lifetime (SubPc)	toluene	0.05 ns	0.041 ns	0.04 ns	0.25 ns
		2.0×10^{10} s^{-1}	2.4×10^{10} s^{-1}	2.5×10^{10} s^{-1}	4.0×10^{-9} s^{-1}
	THF	*b*	*b*	*b*	0.20 ns
					5.0×10^{-9} s^{-1}
	bzcn			0.031 ns	0.16 ns
				3.2×10^{10} s^{-1}	6.25×10^{-9} s^{-1}
singlet excited-state lifetime (C_{60}), ns	toluene	1.39	1.25	1.25	*a*
	THF	1.30		1.29	
	bzcn	1.35	1.21	0.2	
triplet excited-state quantum yield (SubPc)	toluene	0.48	0.43	0.45	
	ODCB	0.43	0.43	0.42	radical pair state
	bzcn	0.43	0.40	0.1	

[a] Masked by the strong SubPc features. [b] Not stable.

the transient bleaching of the *Q*-bands around 560 nm, a new broad transition, which centers around 620 nm.

Fullerene Reference 3. The well-known excited-state properties of fullerene reference **3**, that is, a fulleropyrrolidine, shall be discussed in brief, since they emerge as important reference points for the interpretation of the features seen in dyads **1a**−**d**.[9g] In contrast to SubPcs **2a**−**d**, the fullerene emission is rather weak with a quantum yield of 6×10^{-4}, despite the comparable fluorescence lifetime of ca. 1.5 ns. The singlet excited state, displaying a distinctive singlet−singlet transition around 880 nm, undergoes a quantitative intersystem crossing with a rate of 5×10^{8} s^{-1}. The ISC process yields the long-lived triplet manifold, for which maxima are noted at 360 and 700 nm, followed by a low-energy shoulder at 800 nm.

Dyads 1a−d. The electronic absorption spectra of the SubPc−C_{60} ensembles display common features of each subunit (see Supporting Information). The presence of the fulleropyrrolidine fragment is evidenced by the higher absorption between 250 and 350 nm and in the weak typical band around 430 nm, whereas the macrocyclic unit dominates the red part of the spectrum, its *Q*-band suffering a small bathochromic shift in the dyads.

First, quantitative information on intramolecular deactivation of, for instance, the photoexcited subphthalocyanine chromophore (i.e., excitation at 570 nm) was lent from fluorescence experiments, steady-state and time-resolved. Importantly, when the SubPc fluorescence in dyads **1a**−**d** is compared with that in references **2a**−**d**, a strong decrease in intensity is noted (Figure 6). While we determined quantum yields for **2a**−**d** on the order of 0.5, in **1a**−**d** representative values are typically on the order of $(7.5 \pm 2.5) \times 10^{-4}$; see Table 3. The difference in fluorescing quenching between the individual solvents is marginally small, suggesting intramolecular processes that proceed with nearly activationless kinetics.

Likewise with the fluorescence quantum yields, the SubPc fluorescence lifetimes are noticeably shorter in **1a**−**d** relative to what was seen in **2a**−**d**. Considering both lifetimes and quantum yields, we can approximate the deactivation rates, which correspond to intramolecular events of 10^{10} s^{-1}.

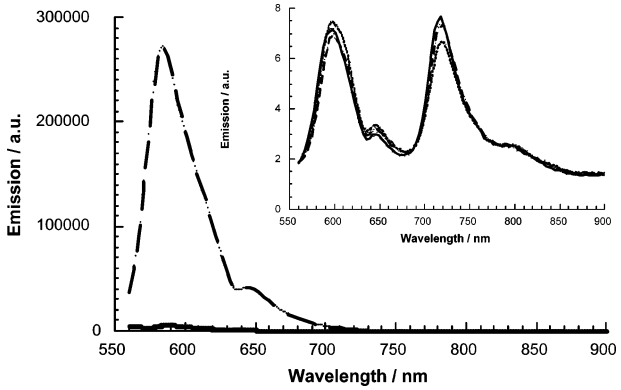

Figure 6. Fluorescence spectra of SubPc **2b** (dashed line) and dyad **1b** (solid line) in toluene with matching absorption at the 570 nm excitation wavelength; $O.D._{570\ nm} = 0.5$. Inset: Fluorescence spectra of dyad **1b** in toluene (solid line), *o*-dichlorobenzene (dashed line), and benzonitrile (dotted line).

Although, at the chosen 570 nm excitation wavelength, the fullerene absorption ($\epsilon_{570\ nm} \approx 2.000$ M^{-1} cm^{-1}) plays an irrelevant role, relative to the strong absorption of the subphthalocyanine ($\epsilon_{570\ nm} \approx 50.000$ M^{-1} cm^{-1}), we noticed, parallel with the reduced SubPc fluorescence, the typical fullerene fluorescence at lower energies, as shown in Figure 6. In particular, in most solvents and most compounds, the 720 nm fingerprint is seen. The determination of the fullerene fluorescence quantum yield, employing **3** as a standard with matching absorption at the excitation wavelength, afforded values that are $\sim 5 \times 10^{-4}$. Since these Φ-values nearly approach that measured for **3**, namely, 6.0×10^{-4}, this process appears to be nearly quantitative. Because of the dominant absorption of the SubPc moiety at the 570 nm excitation wavelength, we gather a highly efficient transduction of singlet excited-state energy from the photoexcited subphthalocyanine to the fullerene.[22]

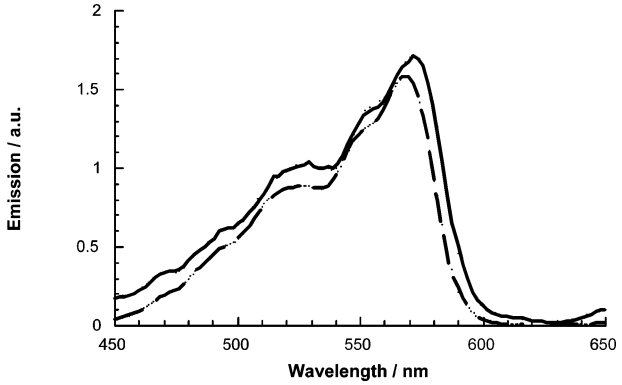

Figure 7. Excitation spectra (normalized to exhibit matching signals around 570 nm) of SubPc **2b** (dashed line) and dyad **1b** (solid line) in toluene monitoring the SubPc emission around 600 nm and the fullerene emission at 720 nm, respectively.

Since the energy transfer process is thermodynamically feasible, we probed excitation spectra of the fullerene emission. In line with our energy transfer hypothesis, the excitation spectrum resembles the ground-state spectrum of the SubPc and the excitation spectrum of the SubPc fluorescence; an illustration is given in Figure 7, displaying the spectra of **2b** and dyad **1b**. In conclusion, the fluorescence assay prompts for dyads **1a**−**c** to a rapid and nearly quantitative transfer of singlet-excited-state energy from the subphthalocyanine (2.1 eV) to the fullerene moiety (1.76 eV).

Exceptions from this trend are dyad **1c** in benzonitrile and dyad **1d** in all the solvents studied. In the earlier case, no fullerene emission was seen at all. In the latter case, the red-shifted SubPc fluorescence extends into the region of the fullerene fluorescence, which, in turn, renders a quantitative and exact quantum yield determination rather difficult. But in comparing the fluorescence ratio at 560 versus 720 (i.e., fluorescence maxima of the SubPc and fullerene core) in reference **2d** and dyad **1d**, we can estimate an upper fluorescence quantum yield ($\Phi < 1.0 \times 10^{-4}$) for the fullerene moiety. Interestingly, the SubPc moiety in dyad **1d** is the best electron donor among those investigated. Thus, we postulate at this point that here an intramolecular electron-transfer process may occur; more details will follow below.

As far as the time-resolved fluorescence decay measurements are concerned, only the fullerene contributions were seen at ~715 nm with fluorescence lifetimes (~1.5 ns) that are, in dyads **1a**−**c**, virtually indistinguishable from those measured for **3**. In other words, once formed, the fullerene singlet excited state decays via the ordinary ISC process. In **1d**, on the other hand, the fullerene fluorescence is much shorter lived, indicating that it decays via a rapid intramolecular electron transfer; see below. Please note that detection of the subphthalocyanine fluorescence was hampered by the instrumental time resolution (<100 ps) for all but **1d**.

In time-resolved transient absorption measurements, an instantaneous grow-in of a 650 nm absorption results from the 532 nm laser irradiation. The similarity of this transition with those noted for the SubPc singlet excited-state features in **2a**−**d** (see Figure 5a) affirms the successful SubPc excitation in the dyads, **1a**−**d**. Instead of seeing, however, the slow ISC dynamics that **2a**−**d** exhibit (~10^8 s^{-1}), the SubPc singlet−singlet absorptions decay when C_{60} is present (i.e., **1a**−**c**) with ultrafast dynamics of $(2 \pm 1) \times 10^{10}$ s^{-1}. The singlet excited-state

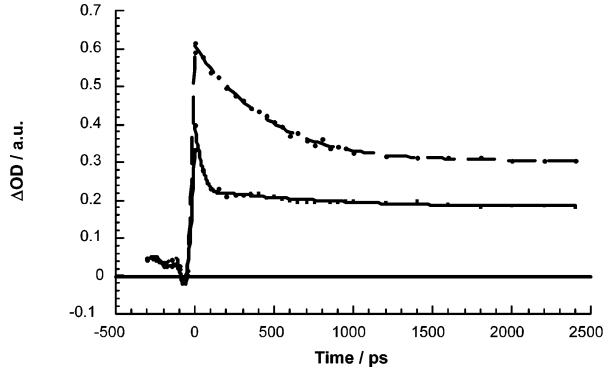

Figure 8. Time-absorption profiles at 650 nm (solid line) and 880 nm (dashed line) of dyad **1b** in nitrogen saturated toluene; the intensity of the solid line is decreased by a factor of 2. The baseline drift in the time window prior to the laser pulse is due to scattering.

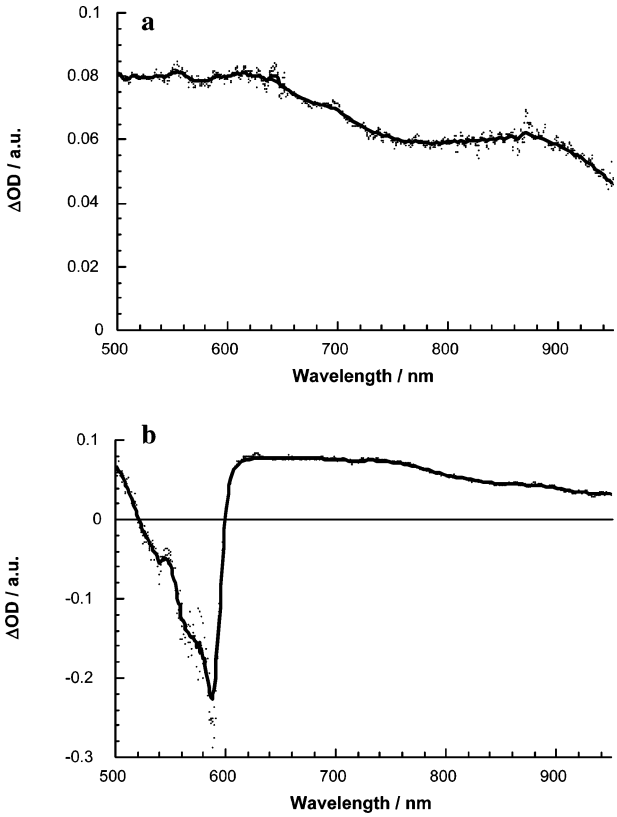

Figure 9. Differential absorption spectra obtained upon picosecond flash photolysis (532 nm) of ~1.0×10^{-5} M solutions of dyad **1b** in nitrogen saturated toluene (a) 50 ps and (b) 2500 ps, showing the fullerene singlet and SubPc triplet excited-state features.

lifetimes, as they were determined from an average of first-order fits of the time-absorption profiles at various wavelengths, are listed in Table 3. An example of the SubPc decay at 650 nm is given in Figure 8. Spectroscopically, the transient absorption changes, taken after the completion of the decay, bear no resemblance with the SubPc triplet excited state (vide supra). In particular, the new transients reveal broad maxima at 880 nm, which match those of the C_{60} singlet−singlet features. Figure 9 illustrates the spectral differences of the two spectra, namely, that of the C_{60} singlet and that of the SubPc triplet for the dyad (i.e., **1b**). An important kinetic aspect is that the SubPc singlet excited state lifetimes match quantitatively those values derived in the fluorescence experiments. This

confirms, spectroscopically and kinetically, the transduction of singlet excited state from the SubPc (2.1 eV) to the C_{60} moiety (1.76 eV).

In reference **3**, and also in other C_{60} derivatives, the deactivation of the singlet excited state is dominated by ISC (5.0×10^8 s^{-1}) to the energetically lower lying triplet. In this regard, it is important to note that, in **1a**−**c**, the 880 nm transition decays with kinetics that are hardly faster ($\sim 8.0 \times 10^8$ s^{-1}) than the inherent ISC dynamics; see Figure 8.

Interestingly, we did not find the characteristic C_{60} triplet features, including a strong triplet−triplet transition at 700 nm with an extinction coefficient of $\sim$15.000 M^{-1} cm^{-1} at the end of the C_{60} singlet deactivation/ISC. On the contrary, a maximum around 620 nm and a minimum at 570 nm were concluded. Earlier we established that such features are reliable attributes of the SubPc triplet excited state. Please note the excellent agreement of the 500−950 nm region in Figures 9b and 5b, showing the SubPc triplet spectra in **1b** and **2b**, respectively. From this we infer that the C_{60} triplet (1.5 eV), once formed, undergoes a thermodynamically allowed transfer of triplet energy to the SubPc triplet (1.45 eV). Nearly, similar kinetics at the 570-nm minimum, which allowed us to follow the generation of the SubPc triplet, further furnishes the following kinetic assignment: the rate-determining step in the SubPc triplet formation is the C_{60} intersystem crossing.

The only component seen in the complementary nanosecond experiments was that of the SubPc triplet ($\lambda_{max} = 460$, 620 nm, $\lambda_{min} = 570$ nm), similar to what is shown in Figure 5b. In addition, high SubPc triplet quantum yields in **1a**−**c**, as determined in a variety of solvents, further confirm the cascade of singlet−singlet and triplet−triplet energy transfer processes, transducing the excitation energy back and forth between the two moieties.

Quite different is the situation for **1d**. While the excited state of **2d** is essentially stable on the picosecond time scale and recovers to the triplet state, the SubPc singlet excited state related features transform in **1d** within 300 ps into a broad absorbing species. The rate constant of $(4.5 \pm 0.5) \times 10^9$ s^{-1} is somewhat slower than what is noted for **1a**−**c**. Again, the kinetics are matching those registered in the fluorescence experiments. The transient product of the rapid singlet deactivation shows maxima at 685 nm, which match those of the one-electron oxidized SubPc radical cations ($SubPc^{\bullet+}$), and 1000 nm, which resembles that of the one-electron reduced C_{60} radical anions ($C_{60}^{\bullet-}$). Collectively, these features confirm the successful generation of $SubPc^{\bullet+}-C_{60}^{\bullet-}$, for which we determined an energy level of approximately 1.4 eV.

The $SubPc^{\bullet+}-C_{60}^{\bullet-}$ transients for **1d** are stable up to the time scale of 100 ns (Figure 10). To examine the charge-recombination dynamics, the spectral fingerprints of $C_{60}^{\bullet-}$ (1000 nm) and that of $SubPc^{\bullet+}$ (685 nm) are useful probes. Important is the fact that the decays of both probes resemble each other and give rise to unimolecular recovery kinetics of the singlet ground state. Relative to the radical pair lifetimes of 145 ns (i.e., in THF) and 101 ns (i.e., ODCB), benzonitrile discloses a further destabilizing trend. In particular, 72 ns is in line with our previous observation on $ZnP^{\bullet+}/C_{60}^{\bullet-}$ radical pairs,[9] which implies charge-recombination deep in the inverted region, since $-\Delta G_{CR}$ becomes gradually less negative in the THF < ODCB < benzonitrile order.

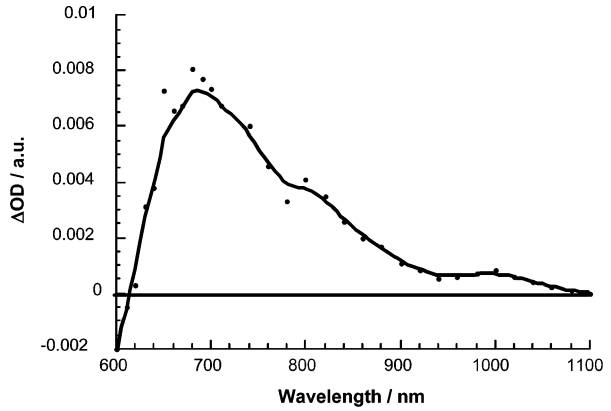

Figure 10. Differential absorption spectrum obtained upon nanosecond flash photolysis (532 nm) of $\sim 1.0 \times 10^{-5}$ M solutions of dyad **1d** in nitrogen saturated benzonitrile with a time delay of 50 ns, showing the radical pair features.

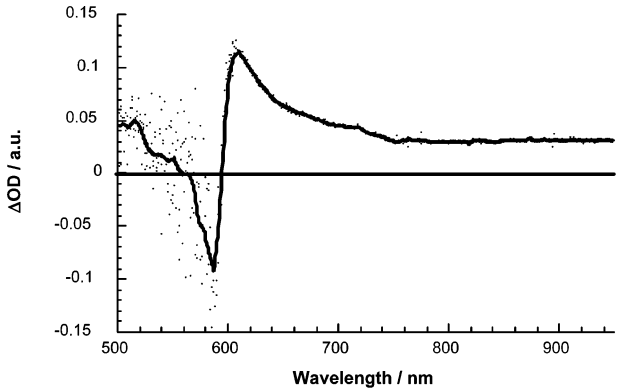

Figure 11. Differential absorption spectrum obtained upon picosecond flash photolysis (532 nm) of $\sim 1.0 \times 10^{-5}$ M solutions of dyad **1c** in nitrogen saturated benzonitrile with a time delay of 50 ps, showing the radical pair features.

Similarly, in dyad **1c** we found the $SubPc^{\bullet+}-C_{60}^{\bullet-}$ radical pair (see Figure 11) as the metastable photoproduct, but only in benzonitrile! From the electrochemical experiments we approximate an $SubPc^{\bullet+}-C_{60}^{\bullet-}$ energy level of ca. 1.65 eV. In line with the fact that the radical pair state is higher than the two triplets, namely, fullerene (1.5 eV) and subphthalocyanine (1.46 eV), we notice at time delays of 2 ns and more only the SubPc triplet features. The triplet grow-in is, however, kinetically linked to the decay of the charge-separated ion pair absorption ($SubPc^{\bullet+}-C_{60}^{\bullet-}$). They follow similar kinetics with a τ of about 0.65 ns. This would signify that the charge-separated state in benzonitrile decays via the energetically lower lying triplet excited state (1.46 eV) with small $-\Delta G_{CR}$ to regenerate the ground state, rather than a direct recombination to the latter.

Summary and Conclusions

In this article, we have introduced subphthalocyanines as novel and promising light-harvesting and/or donor units for artificial photosynthetic systems. For this task, we prepared a series of four SubPc−C_{60} dyads, in which the rational functionalization of the macrocycle by groups of different electronic character provides the means to control the interplay between energy and charge transfer processes. Key to this objective was the development of synthetic routes to SubPcs featuring electron-donating substituents, such as ether or amino groups, which were successfully introduced by condensation of suitable phthalo-

nitrile precursors or by a palladium-catalyzed amination reaction, respectively. The fullerene fragment was attached via the axial position of the macrocycle, which represents a simple and efficient approach to SubPc-based dyads.

The detailed electrochemical and photophysical characterization of the reference SubPc and C_{60} compounds furnished the comprehension and rationalization of the different mechanistic scenarios, energy and electron-transfer deactivation of the photoexcited SubPcs, occurring in the dyads upon initial light irradiation. Cyclic voltammetry experiments revealed the first oxidation process of the macrocycle to gradually shift to lower potentials (by ca. 200 nm) in the series **a** > **b** > **c** > **d**, whereas the first C_{60}-based reduction process remained virtually unaffected. As a consequence, the energy level of the $SubPc^{\bullet+}-C_{60}^{\bullet-}$ charge-separation states are tuned so as to compete with energy transfer deactivation pathways. More specifically, the selective excitation of the SubPc unit in dyads **1a** and **1b**, or in dyad **1c** in a nonpolar environment, gives rise to a sequence of exergonic photophysical events that involve (i) nearly quantitative singlet−singlet energy transfer to the C_{60} moiety, (ii) fullerene centered intersystem crossing, and (iii) triplet−triplet energy transfer back to the SubPc. In fact, the energy level of the overall product, the SubPc triplet excited state, has been for the first time ascertained from phosphorescence measurements around 1.45 eV, just below the fullerene triplet state. On the contrary, the stabilization of the $SubPc^{\bullet+}-C_{60}^{\bullet-}$ radical pair state in more polar media or by lowering the redox gap causes charge transfer to dominate. In the case of **1c** in benzonitrile, the thus formed radical pair has a lifetime of 0.65 ns and decays via the energetically lower lying triplet excited state. Further stabilization is achieved for dyad **1d**, whose charge-transfer state would lie now below both triplets. The radical pair lifetime consequently increases in more than 2 orders of magnitude with respect to **1c** and presents a significant stabilization in less polar solvents, a clear attribute of the inverted region of the Marcus parabola.

In conclusion, we have proven that subphthalocyanines are synthetically and electronically versatile molecular units for the construction of multicomponent photoactive systems. Future research will be aimed at determining the electron-accepting ability of these chromophores in specifically designed dyads.

Experimental Section

General Methods. Melting points (mp) were determined in a Büchi 504392-S equipment and are uncorrected. UV/vis spectra were recorded with a Hewlett-Packard 8453 instrument. IR spectra were recorded on a Bruker Vector 22 spectrophotometer. LSI-MS and HRMS spectra were determined on a VG AutoSpec apparatus, and MALDI-TOF-MS spectra were obtained from a BRUKER REFLEX III instrument equipped with a nitrogen laser operating at 337 nm. NMR spectra were recorded with a BRUKER AC-300 instrument. Elemental analyses were performed with a Perkin-Elmer 2400 CHN equipment. Column chromatography was carried out on silica gel Merck-60 (230−400 mesh, 60 Å), and TLC, on aluminum sheets precoated with silica gel 60 F_{254} (E. Merck). Chemicals were purchased from commercial suppliers and used without further purification. Phthalonitrile **4b** was prepared following a reported procedure.[35]

Electrochemistry. Electrochemical measurements were performed at room temperature in a home-built one-compartment cell with a three-electrode configuration, containing 0.1 M tetrabutylammonium hexafluorophosphate ($TBAPF_6$) as the supporting electrolyte, which was recrystallized twice from ethanol and dried under vacuum. A glassy carbon or gold electrode (3 or 1.5 mm ϕ, respectively) was used as the working electrode, and a platinum mesh and a silver wire, separated from the solution by a Vycor tip, were employed as the counter and the reference electrodes, respectively. Prior to each voltammetric measurement, the cell was degassed and pumped to 10^{-6} mmHg. The solvent, THF (5 mL), which had also been degassed and pumped to the same pressure, was then vapor-transferred into the cell, directly from Na/K. The electrochemical measurements were performed using a concentration of approximately 0.5 mM of the corresponding compound, and ferrocene was added as an internal reference.

Photophysics. Picosecond laser flash photolysis experiments were carried out with 532-nm laser pulses from a mode-locked, Q-switched Quantel YG-501 DP Nd:YAG laser system (18 ps pulse width, 2−3 mJ/pulse). Nanosecond Laser Flash Photolysis experiments were performed with laser pulses from a Quanta-Ray CDR Nd:YAG system (532 nm, 6 ns pulse width) in a front face excitation geometry. Fluorescence lifetimes were measured with a Laser Strobe Fluorescence Lifetime spectrometer (Photon Technology International) with 337 nm laser pulses from a nitrogen laser fiber-coupled to a lens-based T-formal sample compartment equipped with a stroboscopic detector. Details of the Laser Strobe systems are described on the manufacture's web site, http://www.pti-nj.com. Emission spectra were recorded with an SLM 8100 spectrofluorometer. The experiments were performed at room temperature. Each spectrum represents an average of at least five individual scans, and appropriate corrections were applied whenever necessary. Pulse radiolysis experiments were performed by utilizing 50-ns pulses of 8 MeV electrons from a model TB-8/16-1S Electron Linear Accelerator. Details on such equipment, in general, and the data analysis have been described elsewhere.[36]

Dibenzo[*b*,*e*][1,4]dioxine-2,3-dicarbonitrile (4c): In a 100-mL round-bottomed flask, equipped with a magnetic stirrer and rubber seal, 4,5-dichlorophthalonitrile (2.4 g, 12.2 mmol), dry K_2CO_3 (5.0 g, 36.2 mmol), and dry dimethylacetamide (30 mL) were placed. Then, catechol (1.34 g, 12.2 mmol) was added. The resulting mixture was stirred under argon at room temperature for 16 h and at 50 °C during 3 h. After that time, it was poured into 100 mL of cold water, and the precipitate formed was collected by filtration and subjected to column chromatography on silica gel using a 1:1 mixture of CH_2Cl_2/hexane. In this way, 3.2 g (89%) of compound **4c** were isolated as a white solid. Mp: 138−139 °C. ^{1}H NMR (300 MHz, $CDCl_3$): δ = 7.19 (s, 2H), 7.05−6.85 ppm (AA'BB', 4H). ^{13}C NMR (75.5 MHz, $CDCl_3$): δ = 146.0, 140.3, 125.6, 121.4, 116.8, 114.6, 111.6 ppm. MS (EI): m/z = 234 $[M]^+$ (100%). FT-IR (KBr): ν = 3078, 2988 (C−H), 2236 (C≡N), 1616, 1503, 1284, 1242 (C−O), 869, 747 cm^{-1}. Anal. Calcd for $C_{14}H_6N_2O_2$: C, 71.80; H, 2.58; N, 11.96. Found: C, 71.78; H, 2.59; N, 11.93.

Standard Procedure for the Synthesis of SubPcs 5a−c: In a 25-mL two-necked round-bottomed flask, equipped with a condenser, magnetic stirrer, and rubber seal, BCl_3 (5 mL, 1M solution in *p*-xylene) was added to the corrresponding dry phthalonitrile (5 mmol) under argon atmosphere. The reaction mixture was then stirred under vigorous reflux for 20 min, allowed to reach room temperature, and flushed with argon. The dark purple reaction slurry was dissolved in toluene/THF (10:1) and passed through a short silica plug. The solvent was removed by vacuum distillation, and the resulting dark solid was subjected to column chromatography on silica gel using a 3:1 mixture of hexane/ethyl acetate (**5a** and **5c**) or toluene (**5b**) as eluent. Compounds **5a−c** were further purified by recrystallization from CH_2Cl_2/hexane (**5a** and **5b**) or methanol/water (**5c**) mixtures. The characterization of SubPc **5a**[14f] and the C_3 and C_1 regioisomers of SubPc **5b**[15a] has been recently reported.

(35) Marcuccio, M. S.; Polina, I.; Greenberg, S.; Lever, A. B. P.; Leznoff, C. C.; Tomer, B. *Can. J. Chem.* **1985**, *63*, 3057−3069.

(36) Hug, G. L.; Wang, Y.; Schöneich, C.; Jiang, P.-Y.; Fessenden, R. W. *Radiat. Phys. Chem.* **1999**, *54*, 559.

Chloro-[2,3,9,10,16,17-tri(benzo[1,4]dioxine)subphthalocyaninato]-boron (III) (5c). Compound **5c** was obtained as a red solid: 0.49 g (39%). Mp > 250 °C. ^{1}H NMR (300 MHz, $CDCl_3$): δ = 8.23 (s, 6H), 7.05−6.9 ppm (AA′BB′, 12H). ^{13}C NMR (75.5 MHz, $CDCl_3$): δ = 149.1, 145.0, 141.5, 127.4, 124.5, 116.6, 109.2 ppm. MS (FAB, *m*-NBA): *m*/*z* = 749 $[M]^+$, 714 $[M - Cl]^+$. HRMS calcd for $C_{42}H_{18}N_6O_6BCl$: 748.1069; found, 748.1106. UV−vis ($CHCl_3$): λ_{max} (log ϵ) = 574 (4.6), 532 (sh), 408 (3.9), 292 nm (4.5). FT-IR (KBr): ν = 1565, 1490, 1284, 1133, 956 (B−Cl), 870, 742 cm^{-1}. Anal. Calcd for $C_{42}H_{18}N_6O_6BCl$: C, 67.36; H, 2.42; N, 11.22. Found: C, 67.40; H, 2.35; N, 11.30.

Standard Procedure for the Synthesis of SubPcs 2a−c and 6b−c: In a 25-mL round-bottomed flask, equipped with a condenser and a magnetic stirrer, the corresponding phenol (2.5 mmol) and the SubPc (0.5 mmol) were refluxed in toluene (2 mL) for 40 h (**2a**), 16 h (**2b**), 4h (**2c**), 40 h (**6b**), or 9 h (**6c**), depending in each case on the reactivity of the starting SubPc and phenol. The reaction mixture was cooled to room temperature, the solvent was evaporated, and the resulting residue was washed with a 4:1 mixture of methanol/water. The dark magenta solid was then subjected to column chromatography on silica gel using toluene (**2a−c**) or mixtures of toluene/THF (30:1 for **6b** or 20:1 for **6c**). The C_3 and C_1 regioisomers of **2b** were separated during chromatography, and their individual characterization data are listed below following their elution order. Compounds **2a−c** and **6b−c** were further purified by recrystallization from CH_2Cl_2/hexane mixtures. The characterization of SubPcs **2a**[14f] and **6a**[21b] has been recently reported.

Phenoxy-[2,9,16-triiodosubphthalocyaninato]boron (III) (2b; C_3 Isomer). Compound **2b** (***C*$_3$**) was obtained as a magenta solid: 80 mg (20%). Mp > 250 °C. ^{1}H NMR (300 MHz, $CDCl_3$): δ = 9.16 (d, J_m = 1.4 Hz, 3H), 8.50 (d, J_o = 8.2 Hz, 3H), 8.17 (dd, J_o = 8.2 Hz, J_m = 1.4 Hz, 3H), 6.76 (dd, J_o = 8.2 Hz, $J_{o'}$ = 7.1 Hz, 2H), 6.64 (t, $J_{o'}$ = 7.1 Hz, 1H), 5.36 ppm (d, J_o = 8.2 Hz, 2H). ^{13}C NMR (75.5 MHz, $CDCl_3$): δ = 152.1, 151.3, 150.1, 138.8, 132.2, 129.8, 131.4, 129.0, 123.5, 121.8, 119.0, 96.2 ppm. MS (FAB, *m*-NBA): *m*/*z* = 866 $[M]^+$, 773 $[M - \text{axial group}]^+$. UV−vis ($CHCl_3$): λ_{max} (log ϵ) = 573 (4.5), 558 (sh), 530 (sh), 340 (4.0), 317 (4.1), 277 nm (4.2). FT-IR (KBr): ν = 1599, 1439, 1177, 1056 (B−O), 820, 757, 705 cm^{-1}. Anal. Calcd for $C_{30}H_{14}N_6OBI_3$: C, 41.61; H, 1.63; N, 9.70. Found: C, 41.46; H, 1.77; N, 9.54.

Phenoxy-[2,9,17-triiodosubphthalocyaninato]boron (III) (2b; C_1 Isomer). Compound **2b** (***C*$_1$**) was obtained as a magenta solid: 0.28 g (66%). Mp > 250 °C. ^{1}H NMR (300 MHz, $CDCl_3$): δ = 9.15−9.1 (m, 3H), 8.55−8.45 (m, 3H), 8.2−8.1 (m, 3H), 6.77 (dd, J_o = $J_{o'}$ = 7.6 Hz, 2H), 6.64 (t, $J_{o'}$ = 7.6 Hz, 1H), 5.38 ppm (d, J_o = 7.6 Hz, 2H). ^{13}C NMR (75.5 MHz, $CDCl_3$): δ = 152.1, 151.5, 151.3, 151.1, 150.3, 150.2, 150.0, 138.7, 132.3, 132.2, 132.1, 129.9, 129.7, 131.4, 129.0, 123.52, 123.46, 121.8, 119.0, 96.2 ppm. MS (FAB, *m*-NBA): *m*/*z* = 866 $[M]^+$, 773 $[M - \text{axial group}]^+$. HRMS calcd for $C_{30}H_{14}N_6OBI_3$: 865.8456; found, 865.8451. UV−vis ($CHCl_3$): λ_{max} (log ϵ) = 573 (4.6), 558 (sh), 532 (sh), 342 (sh), 317 (4.2), 276 nm (4.3). FT-IR (KBr): ν = 1523, 1428, 1252, 1171, 1063 (B−O), 1036, 807, 753, 699 cm^{-1}. Anal. Calcd for $C_{30}H_{14}N_6OBI_3$: C, 41.61; H, 1.63; N, 9.70. Found: C, 41.55; H, 1.67; N, 9.72.

Phenoxy-[2,3,9,10,16,17-tri(benzo[1,4]dioxine)subphthalocyaninato]-boron (III) (2c). Compound **2c** was obtained as a red solid: 0.32 g (79%). Mp > 250 °C. ^{1}H NMR (300 MHz, $CDCl_3$): δ = 8.18 (s, 6H), 7.05−6.8 (AA′BB′, 12H), 6.78 (dd, J_o = 7.6 Hz, $J_{o'}$ = 8.2 Hz, 2H), 6.64 (t, $J_{o'}$ = 8.2 Hz, 1H), 5.39 ppm (d, J_o = 7.6 Hz, 2H). ^{13}C NMR (75.5 MHz, $CDCl_3$): δ (ppm) = 152.0, 150.4, 144.7, 141.5, 128.9, 127.3, 124.3, 121.5, 119.1, 116.5, 109.0 ppm. MS (FAB, *m*-NBA): *m*/*z* = 806 $[M]^+$, 713 $[M - \text{axial group}]^+$. HRMS calcd for $C_{48}H_{23}N_6O_7B$: 806.1721; found, 806.1700. UV−vis ($CHCl_3$): λ_{max} (log ϵ) = 571 (4.7), 555 (sh), 532 (sh), 401 (4.0), 287 nm (4.7). FT-IR (KBr): ν = 1636, 1568, 1495, 1465, 1389, 1285, 1243, 1133, 1037 (B−O), 866, 810, 747, 704 cm^{-1}. Anal. Calcd for $C_{48}H_{23}N_6O_7B$: C, 71.48; H, 2.87; N, 10.42. Found: C, 71.39; H, 2.97; N, 10.40.

3-Formylphenoxy-[2,9,16(17)-triiodosubphthalocyaninato]-boron (III) (6b; 1:3 Mixture of C_3 and C_1 Isomers). Compound **6b** was obtained as a pink solid: 0.32 g (73%). Mp > 250 °C. ^{1}H NMR (300 MHz, $CDCl_3$): δ = 9.59 (s, 1H), 9.15−9.0 (m, 3H), 8.5−8.35 (m, 3H), 8.2−8.0 (m, 3H), 7.15 (d, J_o = 7.6 Hz, 1H), 6.93 (dd, J_o = $J_{o'}$ = 7.6 Hz, 1H), 5.91 (s (br), 1H), 5.61 ppm (dd, $J_{o'}$ = 7.6 Hz, J_m = 1.2 Hz, 1H). ^{13}C NMR (75.5 MHz, $CDCl_3$): δ = 191.5, 153.0, 151.5, 151.3, 151.1, 150.3, 150.2, 150.1, 149.9, 138.8, 137.3, 132.0, 129.7, 131.5, 131.4, 129.7, 125.2, 123.5, 123.4, 119.6, 96.4 ppm. MS (FAB, *m*-NBA): *m*/*z* = 894 $[M]^+$, 773 $[M - \text{axial group}]^+$. HRMS calcd for $C_{31}H_{14}N_6O_2BI_3$: 893.8405; found, 893.8431. UV−vis ($CHCl_3$): λ_{max} (log ϵ) = 571 (4.6), 530 (sh), 326 (4.0), 273 nm (4.3). FT-IR (KBr): ν = 1694 (C=O), 1598, 1546, 1460, 1436, 1382, 1308, 1266, 1222, 1173, 1141, 1044 (B−O), 968, 816, 777, 752, 701 cm^{-1}. Anal. Calcd for $C_{31}H_{14}N_6O_2BI_3$: C, 41.65; H, 1.58; N, 9.40. Found: C, 41.51; H, 1.65; N, 9.41.

3-Formylphenoxy-[2,3,9,10,16,17-tri(benzo[1,4]dioxine)subphthalocyaninato]boron (III) (6c). Compound **6c** was obtained as a red solid: 0.27 g (65%). Mp > 250 °C. ^{1}H NMR (300 MHz, $CDCl_3$): δ = 9.62 (s, 1H), 8.16 (s, 6H), 7.1−6.7 (m, 14H), 5.92 (s (br), 1H), 5.62 ppm (dd, J_o = 8.2 Hz, J_m = 1.6 Hz, 1H). ^{13}C NMR (75.5 MHz, $CDCl_3$): δ = 191.7, 151.9, 150.4, 144.8, 141.4, 137.2, 129.5, 127.2, 125.6, 125.4, 122.7, 120.1, 116.5, 109.0 ppm. MS (FAB, *m*-NBA): *m*/*z* = 835 $[M]^+$, 713 $[M - \text{axial group}]^+$. HRMS calcd. for $C_{49}H_{23}N_6O_8B$: 834.1670; found, 834.1663. UV−vis ($CHCl_3$): λ_{max} (log ϵ) = 572 (4.6), 533 (sh), 403 (3.9), 288 nm (4.5). FT-IR (KBr): ν = 1698 (C=O), 1636, 1567, 1494, 1465, 1386, 1305, 1283, 1240, 1169, 1132, 1102, 1042 (B−O), 864, 829, 749 cm^{-1}. Anal. Calcd for $C_{49}H_{23}N_6O_8B$: C, 70.52; H, 2.58; N, 10.07. Found: C, 70.36; H, 2.70; N, 10.02.

Standard Procedure for the Synthesis of SubPcs 2d and 6d: An oven-dried 25-mL flask was charged with finely ground Cs_2CO_3 (294 mg, 0.9 mmol), $Pd_2(dba)_3$ (8 mg, 0.009 mmol), BINAP (5.6 mg, 0.009 mmol), diphenylamine (152 mg, 0.9 mmol), and the corresponding SubPc (**2b** or **6b** (1:3 mixture of C_3/C_1 regioisomers); 0.1 mmol). The flask was then purged with argon, and dry toluene (10 mL) was added through a syringe. The mixture was heated to reflux under argon atmosphere with continuous stirring for 8 h in both cases. The solution was cooled to room temperature, diluted with toluene (20 mL), filtered, and concentrated to ca. 2−3 mL. The crude product was then purified by flash chromatography on silica gel using a mixture of hexane/THF (4:1 for **2d** and 3:1 for **6d**) as eluent. The C_3 and C_1 regioisomers of **2d** were separated during chromatography, and their individual characterization data are listed below following their elution order. The resulting deep green solids could be further purified by precipitation from cold hexane.

Phenoxy-[2,9,16-tri(diphenylamino)subphthalocyaninato]-boron(III) (2d; C_3 Isomer). Compound **2d** (***C*$_3$**) was obtained as a green solid: 20 mg (20%). Mp > 250 °C. ^{1}H NMR (300 MHz, $CDCl_3$): δ = 8.52 (d, J_o = 8.8 Hz, 3H), 8.37 (d, J_m = 2.0 Hz, 3H), 7.51 (dd, J_o = 8.8 Hz, J_m = 2.0 Hz, 3H), 7.32 (dd, J_o = $J_{o'}$ = 7.6 Hz, 12H), 7.19 (d, J_o = 7.6 Hz, 12H), 7.13 (t, $J_{o'}$ = 7.6 Hz, 6H), 6.77 (dd, J_o = $J_{o'}$ = 7.6 Hz, 2H), 6.60 (t, $J_{o'}$ = 7.6 Hz, 1H), 5.42 ppm (d, J_o = 7.6 Hz, 2H). ^{13}C NMR (75.5 MHz, $CDCl_3$): δ = 151.0, 150.7, 150.0, 147.3, 132.8, 129.7, 128.8, 125.3, 124.5, 124.3, 124.1, 122.7, 121.0, 118.7, 114.4 ppm. MS (FAB, *m*-NBA): *m*/*z* = 989 $[M]^+$. UV−vis ($CHCl_3$): λ_{max} (log ϵ) = 622 (4.6), 556 (sh), 437 (4.2), 400 (sh), 311 nm (4.6). FT-IR (KBr): ν = 3067, 3010 (C−H), 1592, 1488, 1474, 1326 (C−N), 1272, 1191, 1137, 1056 (B−O), 751, 697 cm^{-1}. Anal. Calcd for $C_{66}H_{44}N_9OB$: C, 80.08; H, 4.48; N, 12.73. Found: C, 79.93; H, 4.61; N, 12.80.

Phenoxy-[2,9,17-tri(diphenylamino)subphthalocyaninato]-boron(III) (2d; C_1 Isomer). Compound **2d** (***C*$_3$**) was obtained as a green solid: 66 mg (67%). Mp > 250 °C. ^{1}H NMR (300 MHz, $CDCl_3$): δ = 8.58 (d, J_o = 8.8 Hz, 1H), 8.57 (d, J_o = 8.8 Hz, 1H), 8.50 (d, J_o = 8.8 Hz, 1H), 8.37 (d, J_m = 1.8 Hz, 1H), 8.32 (d, J_m = 1.8

Hz, 1H), 8.31 (d, J_m = 1.8 Hz, 1H), 7.6−7.45 (m, 3H), 7.4−7.0 (m, 30H), 6.78 (dd, $J_o = J_{o'}$ = 7.6 Hz, 2H), 6.61 (t, $J_{o'}$ = 7.6 Hz, 1H), 5.43 (d, J_o = 7.6 Hz, 2H). ^{13}C NMR (75.5 MHz, $CDCl_3$): δ = 151.5, 150.3, 150.1, 149.8, 149.6, 149.4, 147.33, 147.28, 133.2, 133.0, 132.7, 129.7, 129.65, 129.59, 128.8, 125.4, 125.3, 125.2, 124.6, 124.5, 124.3, 124.2, 124.1, 124.0, 122.9, 122.8, 122.7, 121.0, 118.8, 114.6, 114.5, 114.3 ppm. MS (FAB, *m*-NBA): m/z = 989 $[M]^+$, 896 $[M -$ axial group$]^+$. HRMS calcd. for $C_{66}H_{45}N_9OB$: 990.3840; found, 990.3897. UV−vis ($CHCl_3$): λ_{max} (log ϵ) = 620 (4.6), 554 (sh), 473 (4.2), 428 (4.2), 305 nm (4.7). FT-IR (KBr): ν = 3065, 3010 (C−H), 1601, 1480, 1328 (C−N), 1277, 1183, 1061 (B−O), 830, 751, 697 cm^{-1}. Anal. Calcd for $C_{66}H_{44}N_9OB$: C, 80.08; H, 4.48; N, 12.73. Found: C, 80.02; H, 4.57; N, 12.75.

3-Formylphenoxy-[2,9,16(17)-tri(diphenylamino)subphthalocyaninato]boron(III) (6d; 1:3 Mixture of C_3 and C_1 Isomers). Compound **6d** was obtained as a green solid: 83 mg (82%). Mp > 250 °C. ^{1}H NMR (300 MHz, $CDCl_3$): δ = 9.62 (s, 1H), 8.6−8.5 (m, 3H), 8.45−8.25 (m, 3H), 7.6−7.45 (m, 3H), 7.4−7.0 (m, 31H), 6.94 (dd, $J_o = J_{o'}$ = 7.6 Hz, 1H), 5.99 (s (br), 1H), 5.64 ppm (d, $J_{o'}$ = 7.6 Hz, 1H). ^{13}C NMR (75.5 MHz, $CDCl_3$): δ = 191.9, 153.8, 152.3, 151.5, 150.9, 150.6, 150.4, 150.2, 150.1, 150.0, 149.9, 147.3, 147.22, 147.17, 137.2, 133.1, 132.9, 132.6, 129.7, 129.5, 125.4, 125.3, 125.2, 125.1, 124.3, 124.2, 124.1, 122.9, 122.8, 122.7, 122.4, 120.6, 114.4, 114.3, 114.2, 114.1. MS (FAB, *m*-NBA): m/z = 1018 $[M + H]^+$. HRMS calcd for $C_{67}H_{45}N_9O_2B$: 1018.3789; found, 1018.3768. UV−vis ($CHCl_3$): λ_{max} (log ϵ) = 624 (4.6), 580 (sh), 428 (4.3), 301 (4.8) nm. FT-IR (KBr): ν = 1697 (C═O), 1614 (C═N), 1490, 1260, 1194, 1150, 1041 (B−O), 756, 702 cm^{-1}. Anal. Calcd for $C_{67}H_{44}N_9O_2B$: C, 79.05; H, 4.36; N, 12.38; C, 78.98; H, 4.41; N, 12.34.

Standard Procedure for the Synthesis of SubPc−C_{60} Dyads 1a−d: A dry toluene solution (50 mL) of C_{60} fullerene (70 mg, 0.1 mmol), *N*-methylglycine (25 mg, 0.27 mmol), and the corresponding (formylphenoxy)SubPc **6a**−**d** (0.09 mmol) was heated to reflux under argon atmosphere for 20 h. The solution was then cooled to room temperature and concentrated under vacuum until ca. 10 mL. The resulting mixture was poured onto a silica gel column and eluted with the corresponding solvent mixture to separate the monoaddition products from the bisadducts and unreacted fullerene. The C_3 and C_1 regioisomers of **1b** and **1d** were separated during chromatography, and their individual characterization data are listed below following their elution order. Further purification of the monoadducts was achieved by thoroughly washing the solid products with acetone, methanol, and hexane.

3-(1-Methyl-3,4-[60]fulleropyrrolidin-2-yl)phenoxy-[1,2,3,4,8,9,10,11,15,16,17,18-dodecafluorosubphthalocyaninato]boron(III) (1a). Compound **1a** was obtained as a purple solid: 58 mg (44%). Mp > 250 °C. ^{1}H NMR (300 MHz, $CDCl_3/CS_2$ (1:5)): δ = 7.1−6.9 (m, 1H), 6.81 (dd, $J_o = J_{o'}$ = 7.6 Hz, 1H), 5.9−5.7 (m, 1H), 5.34 (d (br), J_o = 7.6 Hz, 1H), 4.94 (d (br), ^2J = 9.4 Hz, 1H), 4.56 (s (br), 1H), 4.16 (d, ^2J = 9.4 Hz, 1H), 2.73 nm (s, 3H). ^{13}C NMR (75.5 MHz, $CDCl_3/CS_2$ (1:5)): δ = 155.5, 153.2, 153.1, 152.5, 152.4, 151.6, 151.1, 148.0, 146.8, 146.0, 145.9, 145.7, 145.62, 145.57, 145.2, 145.1, 145.0, 144.9, 144.8, 144.7, 144.5, 144.3, 144.2, 144.0, 143.9, 143.8, 143.6, 142.7, 142.6, 142.3, 142.2, 142.1, 141.73, 141.67, 141.51, 141.46, 141.4, 141.3, 141.2, 141.1, 141.0, 140.81, 140.76, 140.7, 140.61, 140.59, 140.56, 140.4, 140.3, 140.1, 139.9, 139.8, 139.7, 139.5, 139.3, 138.8, 138.6, 138.2, 135.8, 135.5, 135.31, 135.26, 152.5, 148.0, 138.8, 128.8, 122.9, 118.1, 115−0−114.4, 110.1, 82.2, 69.5, 68.4, 39.5 ppm. MS (MALDI-TOF, dithranol): m/z = 1478−1483 $[M + H]^+$. UV−vis ($CHCl_3$): λ_{max} (log ϵ) = 573 (4.6), 529 (sh), 430, 316 (4.5), 260 nm (4.8). FT-IR (KBr): ν = 1462, 1395, 1273, 1139, 1044 (B−O), 869, 743 cm^{-1}. Anal. Calcd for $C_{93}H_{10}N_7OF_{12}B$: C, 75.48; H, 0.68; N, 6.63; C, 75.26; H, 0.71; N, 6.57.

3-(1-Methyl-3,4-[60]fulleropyrrolidin-2-yl)phenoxy-[2,9,16-triiodosubphthalocyaninato]boron (III) (1b; C_3 Isomer; 1:1 Mixture of Diastereoisomers). Compound **1b (C_3)** was obtained as a dark red solid: 17 mg (12%). Mp > 250 °C. ^{1}H NMR (300 MHz, $CDCl_3/CS_2$ (1:5)): δ = 9.2−9.1 (m, 3H), 8.6−8.4 (m, 3H), 8.25−8.05 (m, 3H), 7.1−6.8 (m, 1H), 6.8−6.7 (m, 1H), 5.85−5.6 (m, 1H), 5.4−5.25 (m, 1H), 4.95−4.8 (m, 1H), 4.55−4.4 (m, 1H), 4.08 (d, ^2J = 9.2 Hz, 1H), 2.57 ppm (s, 3H). MS (MALDI-TOF, dithranol): m/z = 1641−1646 $[M + H]^+$. UV−vis ($CHCl_3$): λ_{max} (log ϵ) = 573 (4.5), 524 (sh), 432, 322 (4.4), 260 nm (4.8). FT-IR (KBr): ν = 2965, 2922, 1628, 1451, 1346, 1275, 1059 cm^{-1} (B−O). Anal. Calcd for $C_{93}H_{19}N_7OBI_3$: C, 68.04; H, 1.17; N, 5.97. Found: C, 67.81; H, 1.22; N, 6.03.

3-(1-Methyl-3,4-[60]fulleropyrrolidin-2-yl)phenoxy-[2,9,17-triiodosubphthalocyaninato]boron (III) (1b; C_1 Isomer; 1:1 Mixture of Diastereoisomers). Compound **1b (C_1)** was obtained as a dark red solid: 51 mg (35%). Mp > 250 °C. ^{1}H NMR (300 MHz, $CDCl_3/CS_2$ (1:5)): δ = 9.2−9.0 (m, 3H), 8.6−8.4 (m, 3H), 8.25−8.1 (m, 3H), 7.1−6.8 (m, 1H), 6.8−6.7 (m, 1H), 5.85−5.6 (m, 1H), 5.4−5.25 (m, 1H), 4.95−4.8 (m, 1H), 4.55−4.45 (m, 1H), 4.10 (d, ^2J = 9.4 Hz, 1H), 2.57 ppm (s, 3H). ^{13}C NMR (75.5 MHz, $CDCl_3/CS_2$ (1:5)): δ = 153.3, 152.7, 152.50, 152.49, 151.9, 151.3, 151.2, 151.15, 151.10, 151.05, 150.2, 150.1, 150.0, 149.9, 149.1, 146.6, 146.5, 145.7, 145.6, 145.52, 145.46, 145.39, 145.32, 145.2, 145.14, 145.11, 144.85, 144.81, 144.7, 144.54, 144.51, 144.0, 143.7, 143.6, 142.4, 142.3, 141.9, 141.72, 141.69, 141.6, 141.5, 141.42, 141.36, 141.32, 141.2, 141.1, 140.9, 140.83, 140.79, 139.5, 139.2, 137.6, 136.0, 135.1, 138.5, 132.0, 131.63, 131.58, 129.6, 128.6, 123.4, 123.3, 122.0, 118.6, 109.0, 97.0, 96.8, 82.4, 69.5, 68.4, 39.5 ppm. MS (MALDI-TOF, dithranol): m/z = 1641−1646 $[M + H]^+$. UV−vis ($CHCl_3$): λ_{max} (log ϵ) = 573 (4.5), 522 (sh), 431, 322 (4.4), 260 nm (4.8). FT-IR (KBr): ν = 2964, 2920, 1628, 1449, 1345, 1280, 1059 cm^{-1} (B−O). Anal. Calcd for $C_{93}H_{19}N_7OBI_3$: C, 68.04; H, 1.17; N, 5.97. Found: C, 67.90; H, 1.24; N, 6.08.

3-(1-Methyl-3,4-[60]fulleropyrrolidin-2-yl)phenoxy-[2,3,9,10,16,17-tri(benzo[1,4]dioxine)subphthalocyaninato]boron(III) (1c). Compound **1c** was obtained as a purple solid: 65 mg (46%). Mp > 250 °C. ^{1}H NMR (300 MHz, $CDCl_3/CS_2$ (1:5)): δ = 8.08 (s, 6H), 7.0−6.8 (m, 13H), 6.73 (dd, J_o = 7.6 Hz, $J_{o'}$ = 7.6 Hz, 1H), 5.8−5.6 (m, 1H), 5.32 (d (br), J_o = 7.1 Hz, 1H), 4.87 (d (br), ^2J = 9.4 Hz, 1H), 4.49 (s (br), 1H), 4.09 (d, ^2J = 9.4 Hz, 1H), 2.61 ppm (s, 3H). ^{13}C NMR (75.5 MHz, $CDCl_3/CS_2$ (1:5)): δ = 155.4, 153.4, 152.8, 152.7, 152.5, 150.0, 146.6, 146.5, 146.1, 145.8, 145.6, 145.5, 145.4, 145.3, 145.2, 145.0, 144.8, 144.7, 144.5, 144.4, 144.3, 144.0, 143.9, 143.6, 143.5, 142.3, 142.2, 141.9, 141.8, 141.7, 141.5, 141.4, 141.3, 141.1, 141.0, 140.9, 139.4, 139.2, 138.8, 137.3, 136.1, 136.0, 135.2, 135.1, 128.7, 127.0, 124.1, 121.8, 118.6, 116.3, 109.0, 108.9, 82.4, 69.5, 68.3, 39.4 ppm. MS (MALDI-TOF, dithranol): m/z = 1580−1586 $[M + H]^+$. UV−vis ($CHCl_3$): λ_{max} (log ϵ) = 573 (4.6), 529 (sh), 430, 256 nm (5.0). FT-IR (KBr): ν = 1621, 1450, 1345, 1280, 1187, 1065 cm^{-1} (B−O). Anal. Calcd for $C_{111}H_{28}N_7O_7B$: C, 84.26; H, 1.78; N, 6.20. Found: C, 84.11; H, 1.83; N, 6.17.

3-(1-Methyl-3,4-[60]fulleropyrrolidin-2-yl)phenoxy-[2,9,16-tri(diphenylamino)subphthalocyaninato]boron(III) (1d; C_3 Isomer; 1:1 Mixture of Diastereoisomers). Compound **1d (C_3)** was obtained as a dark red solid: 19 mg (12%). Mp > 250 °C. ^{1}H NMR (300 MHz, $CDCl_3$): δ = 8.49, 8.47 (2xd, J_o = 8.6 Hz, 3H), 8.4−8.3 (m, 3H), 7.5−7.4 (m, 3H), 7.4−7.0 (m, 31H), 6.8−6.65 (m, 1H), 5.8−5.7 (m, 1H), 5.45−5.25 (m, 1H), 4.9−4.7 (m, 1H), 4.45 (s (br), 1H), 4.06, 4.04 (2xd, ^2J = 9.2 Hz, 1H), 2.56, 2.50 ppm (2xs, 3H). MS (MALDI-TOF, dithranol): m/z = 1763−1768 $[M + H]^+$. UV−vis ($CHCl_3$): λ_{max} (log ϵ) = 626 (4.6), 584 (sh), 433 (4.2), 308 (4.9), 258 nm (5.0). FT-IR (KBr): ν = 2949, 2917, 1595, 1480, 1455, 1277, 1185, 1050 (B−O), 751, 700 cm^{-1}. Anal. Calcd for $C_{129}H_{49}N_{10}OB$: C, 87.75; H, 2.80; N, 7.93. Found: C, 87.49; H, 2.82; N, 7.88.

3-(1-Methyl-3,4-[60]fulleropyrrolidin-2-yl)phenoxy-[2,9,17-tri(diphenylamino)subphthalocyaninato]boron(III) (1d; C_1 Isomer; 1:1 Mixture of Diastereoisomers). Compound **1d (C_1)** was obtained as a dark red solid: 52 mg (33%). Mp > 250 °C. ^{1}H NMR (300 MHz, $CDCl_3$): δ = 8.55−8.4 (m, 3H), 8.4−8.25 (m, 3H), 7.5−7.35 (m, 3H), 7.35−7.05 (m, 31H), 6.75−6.6 (m, 1H), 5.95−5.55 (m, 1H), 5.45−5.2 (m, 1H), 4.9−4.65 (m, 1H), 4.40 (s (br), 1H), 4.00 (d (br), ^2J =

9.2 Hz, 1H), 2.52, 2.50 ppm (2xs, 3H). ^{13}C NMR (75.5 MHz, $CDCl_3$): δ = 155.8, 155.7, 153.4, 153.3, 153.2, 151.9, 151.8, 151.1, 151.0, 150.2, 150.0, 149.7, 149.6, 149.4, 149.33, 149.27, 148.7, 148.5, 147.3, 147.2, 147.1, 146.3, 146.1, 146.0, 145.6, 145.5, 145.3, 145.2, 145.0, 144.9, 144.8, 144.73, 144.68, 144.5, 144.4, 144.0, 143.8, 143.2, 142.3, 142.0, 141.6, 141.4, 141.34, 141.29, 141.17, 141.0, 140.9, 140.6, 139.3, 139.2, 139.0, 138.9, 137.6, 136.2, 136.1, 135.1, 135.0, 133.6, 133.4, 133.0, 129.8, 129.7, 128.7, 125.6, 125.4, 125.3, 124.7, 124.6, 124.4, 124.2, 124.1, 123.2, 123.1, 123.0, 122.0, 115.7, 114.5, 114.4, 114.3, 111.8, 82.8, 69.5, 68.5, 39.7 ppm. MS (MALDI-TOF, dithranol): m/z = 1763−1768 $[M + H]^+$. UV−vis ($CHCl_3$): λ_{max} (log ϵ) = 626 (4.6), 566 (sh), 432 (4.2), 308 (5.0), 258 nm (5.2). FT-IR (KBr): ν = 1594, 1449, 1273, 1179, 1098, 1044 (B−O), 805, 751, 697 cm^{-1}. Anal. Calcd for $C_{129}H_{49}N_{10}OB$: C, 87.75; H, 2.80; N, 7.93. Found: C, 87.56; H, 2.85; N, 7.90.

Acknowledgment. The authors are grateful for the financial support of the CICYT (Spain), Comunidad de Madrid and the European Union through grants BQU2002-04697, 07N/0030/2002, and HPRN-CT-2000-0127, respectively (T.T.). This work was also partially supported by the U.S. National Science Foundation, grant CHE-0135786 (L.E.), and the Office of Basic Energy Sciences of the U.S. Department of Energy (D.G.). This is document 4524 from the Notre Dame Radiation Laboratory.

Supporting Information Available: Phosphorescence emission spectrum, differential absorption spectrum of the SubPc radical cation, ^{1}H NMR, ^{13}C NMR and UV−vis spectra of dyads **1a**−**d,** reference compounds **2a**−**d** and **3** and SubPcs **6a**−**d** and complete assignment of NMR signals. This material is available free of charge via the Internet at http://pubs.acs.org.

JA039883V